METASTABLE STRUCTURES IN ALLOYS RAPIDLY COOLED FROM THE MELT

Thesis by
William Klement Jr.

In Partial Fulfillment of the Requirements
For the Degree of
Doctor of Philosophy

California Institute of Technology
Pasadena, California
1962

ACKNOWLEDGMENTS

Professor P. E. Duwez conceived much of the technique herein developed, suggested several experiments and supervised the research. R. H. Willens contributed many valuable suggestions concerning the experiments and designed the low temperature camera. Professor F. S. Buffington carefully read the manuscript.

H.-L. Luo assisted with much of the work. Also contributing to the experiments were A. Abu-Shumays, C.-C. Chao, R. Curtis, M. Malcolm, W. L. Shanks and F. Youngkin.

Fellowships from the National Science Foundation were held during the academic years 1960-1 and 1961-2.

ABSTRACT

Small amounts of liquid alloys are cooled to the solid state very rapidly by means of a technique which is described in detail. Procedures for studying the resultant thin, irregular foils are discussed; most of the results are obtained from x-ray diffraction experiments. Among the non-equilibrium structures found in various alloys are cited the metastable solid solutions in silver-copper and gallium antimonide-germanium alloys, the extended primary solid solutions in some silver-base alloys, and the metastable hexagonal close-packed structures in silver-germanium alloys. The quenching technique is discussed and tentative criteria for the prediction and rationalization of certain metastable structures in alloy systems are inferred from an analysis of the process.

TABLE OF CONTENTS

I. INTRODUCTION

This thesis is concerned with the study of the very rapid cooling and solidification of molten materials, especially metallic alloys, by means of newly developed techniques. Since this work is to be considered as exploratory, some effort is expended to delineate the important physical factors involved in the quenching technique. Of special interest is the attainment of metastable phases, which here means those phases which do not exist at equilibrium at any temperature for the given composition, which tend to equilibrium sufficiently slowly to permit study, and which are not readily obtained with ordinary methods.

Although these metastable phases are of considerable interest, little discussion of their broad significance is given in this thesis. Rather, an attempt is made to elucidate the conditions necessary for their formation so as to develop criteria for their occurrence in other alloy systems. This goal necessitates an examination of the solidification process beginning with the melt and ending with the solid specimen at ambient temperature. Examples of the different classes of metastable structures obtained with the present techniques are presented and discussed.

II. EXPERIMENTAL PROCEDURES

A. PERSPECTIVE

Solidification is most assuredly a rate-dependent process, with the structure and properties of the resultant solid sensitive to the time variation of temperature. At low rates of temperature change, equilibrium thermodynamics usually suffices for an adequate description of the process. The extensive collection of experimental facts available permits a reasonable understanding of the situation, despite the various theoretical difficulties. At somewhat higher rates of cooling, additional factors enter the picture; in addition to the expected theoretical shortcomings, data are scattered and often contradictory. The speculation increases accordingly, with this trend continued into the area of yet higher cooling rates where the experimental data are scanty.

This field of yet higher cooling rates is of interest not only for the sake of curiosity but also in the hope that elucidation of some of the phenomena occurring under normal conditions might result. The effects of such great cooling rates on the liquid to solid transformation have not been much investigated previously because such cooling rates are difficult to obtain.

Only small amounts of the liquid can be cooled rapidly, making measurements during the solidification more difficult.

One must, in general, be satisfied with studying the resultant solid (which may be quite tolerable because of its own interesting features) and trying to work back to gain some insight into the solidification mechanisms. The problem of obtaining high cooling rates is that of promoting heat transfer between a small amount of liquid and a medium at a lower temperature.

The possibilities for several media are examined. Radiative heat transfer is usually much too small at the temperatures of interest. Convective heat transfer is greatest in a stream of rapidly moving gas. The difficulty here is that the liquid droplet disintegrates into globules too small for convenient examination after being subjected to the gas blast. For liquids which are commonly used as quenching media, efficient heat transfer is limited by the vapor layer which builds up around the sample. Liquid metals with very high boiling points and consequent low vapor pressures at the temperatures of interest, e.g., gallium, prove to be reactive chemically and thus inappropriate. Aqueous solutions seem to be the most efficient liquid coolants[1]. If the liquid of interest is shot into a liquid in an effort to minimize the limiting effects of the ubiquitous vapor layer, the projectile disintegrates.

To utilize the high thermal conductivities of appropriate solids, the liquid must be maintained in intimate contact with the solid and spread into as thin a layer as possible. This principle is the raison d'etre for the technique described in this thesis and has been also realized by at least two other groups, Falkenhagen and Hofmann [2], and Salli and his coworkers at Dnepropetrovski State University [3].

Falkenhagen and Hofmann [2] constructed a small conical copper chamber with a tube leading into the vertex and a vacuum connection in the base. With a foil stuck with wax onto the external end of the tube, the chamber was evacuated, and often cooled in liquid nitrogen. The end of the tube was put into a pot of the molten alloy of interest and the wax melted, allowing the molten material to shoot up against the base of the conical chamber and solidify. Fairly large amounts of alloy were involved (e.g.,~20 g of aluminum) and it was then possible to follow the temperature change with time via thermocouples and a fast recording oscillograph. Cooling rates up to 29,000°C/sec were claimed. The solidified materials were then examined by standard techniques such as x-ray diffraction, metallography, etc.

Salli [3] experimented with a device in which the alloy of interest was melted on the end of a catapult by resistance heating. When the catapult was sprung, the molten material

was flung into the crotch of two converging copper plates where films of varying thickness (down to ~ 20μ for iron) were obtained. Cooling rates of $\sim 10^5$ °C/sec were claimed. Sufficient quantitites of the quenched alloys were available for metallographic examinations.

Recently discovered was a patent [4] for a device designed to produce very thin filaments from molten alloys. It is probably superior to the two devices just described and may even be equivalent to the present technique insofar as the rapid cooling and solidification of molten alloys is concerned, although not primarily intended for such a purpose.

B. QUENCHING TECHNIQUES

The present technique requires that a small amount of the material of interest be melted in a nonreactive environment, then ejected onto a substrate of high thermal conductivity held at a lower temperature so that the liquid spreads into a thin layer which cools and solidifies very quickly.

a. Model I

For the first model to be put into extended operation, "Model I" (Fig. 1), alloy charges were melted in graphite or alumina within graphite. The crucibles or "nozzles," as shown in Fig. 2, were designed and machined with a minimum of stress concentrations to avoid failures from the shock waves used to eject the molten alloy. With helium as the driving gas, shock waves were generated by the ruptures of

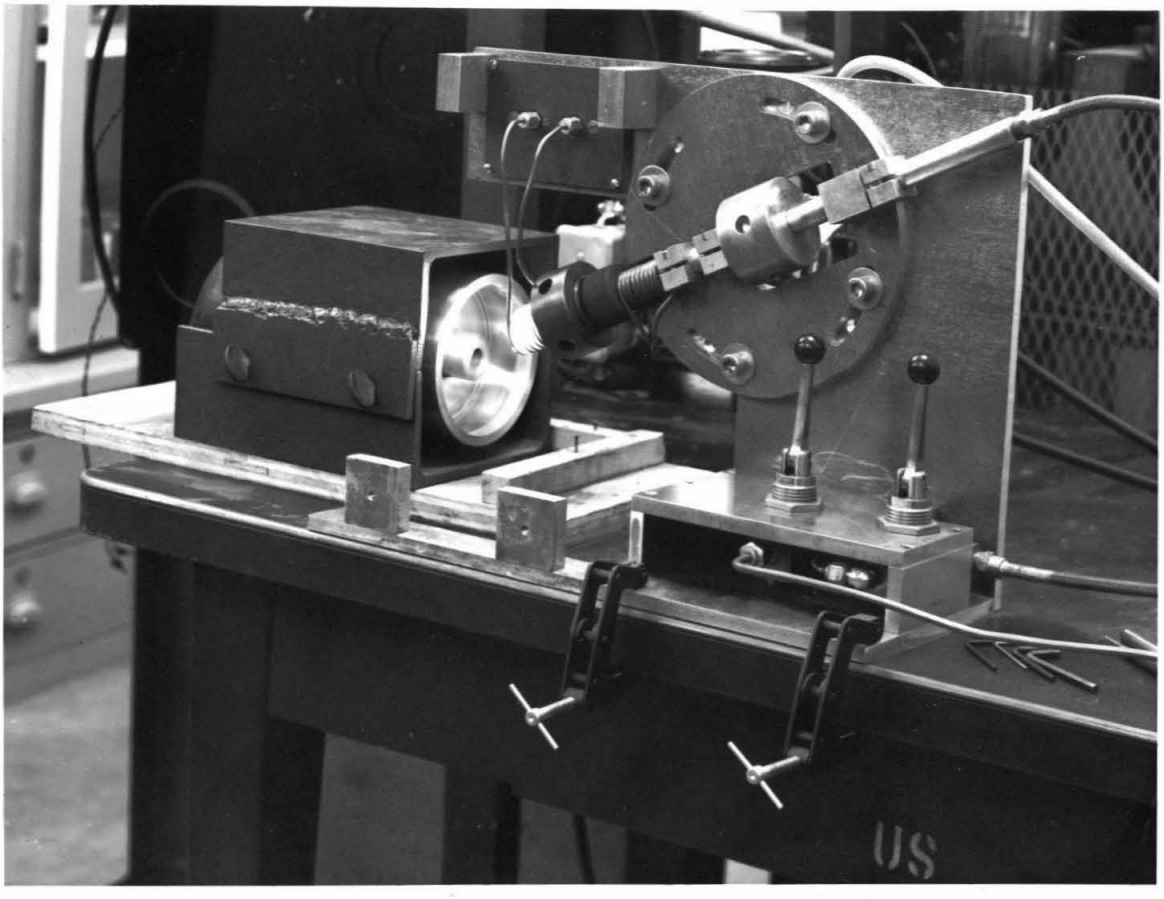

Figure 1. Photograph of Model I.

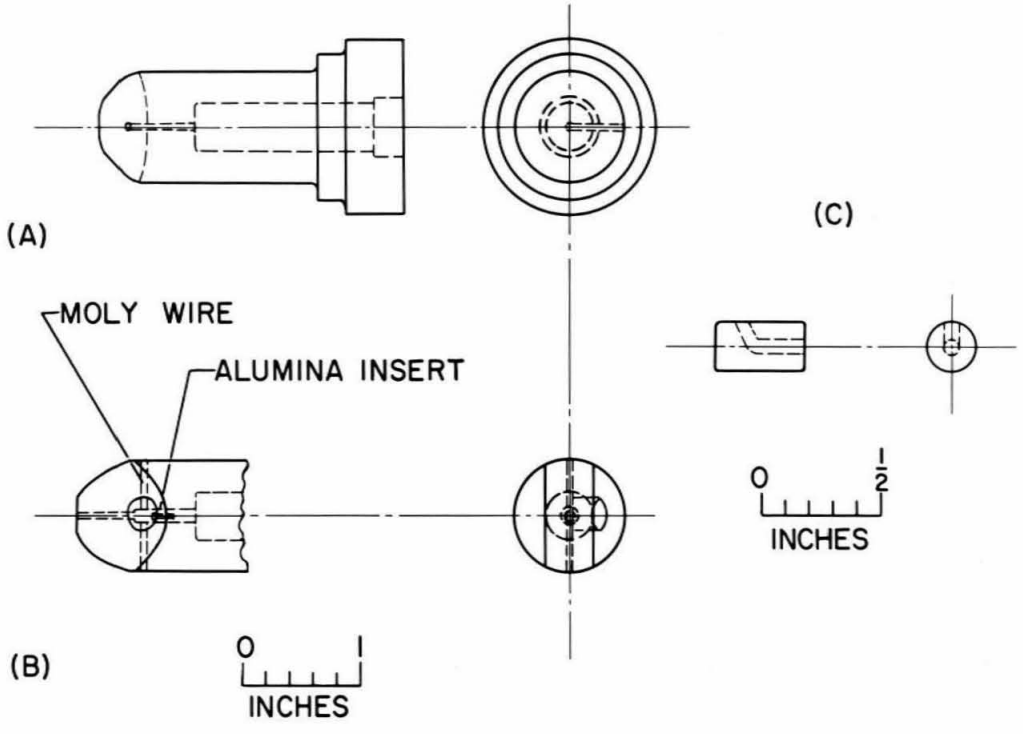

Figure 2. Scaled drawings of graphite nozzle (a), graphite nozzle with alumina insert (b) and alumina insert (c).

mylar diaphragms. Nozzles were heated to 1400°C by eddy currents from rf current supplied to the watercooled induction coil. The criteria [5] for optimum conditions for induction heating were considered in the design of the nozzle.

Strips, onto which the alloys were shot, were mounted on the inner periphery of a rotating wheel. Copper and aluminum were used, with the surface treatments described in II.B.c.

b. Model II

The second model (Fig. 3) was mounted in a dry box to allow the substrate to be maintained at low temperatures without ice formation. Liquid nitrogen was pumped into the box and used for cooling the wheel; the low temperature camera (II.D.)was shuttled through an interchange box mounted below.

The apparatus is closely related to Model I, except that a quick-opening solenoid valve which generated gas pulses was used instead of the diaphragm arrangement. Also, additional cooling was required since temperatures to 1800°C were possible.

c. Discussion

Consider first an alloy wire loaded into a crucible, either graphite or an alumina insert within graphite. As the nozzle was heated by joule losses from eddy currents

Figure 3. Photograph of Model II.

induced by the rf field, the alloy was heated by conduction and radiation. Upon melting, the charge was assumed to move into a stable configuration at the intersection of the holes, completely filling the cross-section. The temperature of the molten alloy was taken to be sensibly that of the surrounding media for graphite crucibles but somewhat lower for the alumina inserts. Temperatures were determined near the hole-surface intersection for graphite nozzles and near the hole for alumina inserts to within $\pm$ 15°C with an L & N optical pyrometer.

Stirring by convection currents should have been sufficient to attain sensible bulk equilibrium within the molten alloys. It was assumed, in general, that the liquids did not wet the crucible, in the sense of spreading along the inner surfaces. Both graphite and alumina have relatively low surface energies and it was unlikely that any wetting took place, in the absence of definite chemical reactions. Only tellurium showed any tendency to wet graphite, and its surface energy is very low compared to the other materials investigated. In the absence of wetting or chemical reactions, it was reasonable to assume that all of the charge was expelled during the shot. Only for tellurium was it observed that some material was ejected during the flush of the gas after a shot.

Operations with reactive liquids and solids at elevated temperatures are subject to contamination. However, in

exploratory work, it is useful to proceed in such a way as to determine what further measures, if any, must be taken to obtain results of the desired quality. Reasonable precautions were taken throughout this work to avoid contaminants and it is believed that the results obtained were not dependent upon such agents.

Assuming that the alloys were not contaminated during preparation, attention must be directed primarily to their melting in the crucibles prior to a shot. For those elements known to react appreciably with carbon, alumina inserts were used. Reactions with nitrogen and oxygen were ever present possibilities but the quenching procedure, especially the melting and firing of the alloy charge, was conducted with reasonable speed and at temperatures no greater than deemed necessary in order to minimize the deleterious reactions. It may be argued that a layer of CO from the erosion of the nozzle partially shielded the melt from the more reactive gases. For reactive metals, such as iron (however, see App. I), the downstream side of the Model II shock tube was filled with helium by repeatedly discharging the solenoid valve and the nozzle, the insert, and surrounding area were thoroughly doused with argon. For Model II operating in a closed dry box, the oxygen was soon consumed.

Considerable variation in the mode of expulsion of the molten droplet is possible. The maximum dynamic pressure associated with the shock wave in Model I may have been about

20,000 psi, as crudely estimated from the nozzle geometry, elastic constants of graphite and the occasional failures in shear. The choices of driving and driven gases probably were not critical.

No measurements of the velocities of the moving droplets were made, but estimates of a few hundred ft/sec. may be reasonable. The dynamics of the moving droplet are rather obscure and all that was absolutely clear was that, under certain conditions, the droplet disintegrated before it hit the target. This situation was readily identified by the incoherence of a specimen in which several droplets impinged and solidified at different times. There is some evidence that it was more difficult to obtain coherent specimens for droplets ejected from graphite nozzles with badly eroded holes. It would seem to be advantageous to have a well defined edge to the hole. Similarly, coherent specimens were more difficult to obtain for alloys shot from the inserts. The length of the hole through which the droplet was accelerated is probably more important here. Disintegration of the speeding droplet may have been due to unstable oscillations initiated by the propelling shock wave or gas pulse and abetted by the crucible geometry and roughness of the hole. On the other hand, air friction may be important. A modification of the technique to operate in vacuo would be useful in assessing the relative importance of the air as well as for some of the spreading effects

described below. The interest in preventing disintegration of the droplet in flight arises from a desire to obtain good spreading and high cooling rates, since there is some evidence that coherent specimens were thinner than incoherent ones, for the same alloy.

The nozzle and rotating wheel were arranged so that the molten droplet would strike the substrate at a grazing angle with the respective velocities approximately additive, i.e., the alloy charge was shot nearly tangentially against the rotating wheel. The rationale behind this geometry was that the molten alloy would be spread into a thinner layer, with consequently higher cooling rates, and this seemed to be borne out in practice.

Distinction between two more or less independent mechanisms must be made for the droplet impinging on the target; viz., spreading of the molten layer and adhesion to the substrate after solidification. The former seems to be related to the surface energies of the molten materials and a brief summary of the pertinent knowledge in this area, gathered mostly from the reviews of Taylor [6] and Bondi [7], is given first.

The liquid-gas surface energies, σ_{LG} , and their variations with temperature have been measured or estimated for many pure metals near their melting points; Fig. 4 shows approximate plots of σ_{LG} vs temperature, with extrapolations for the undercooled liquids. Upon alloying,

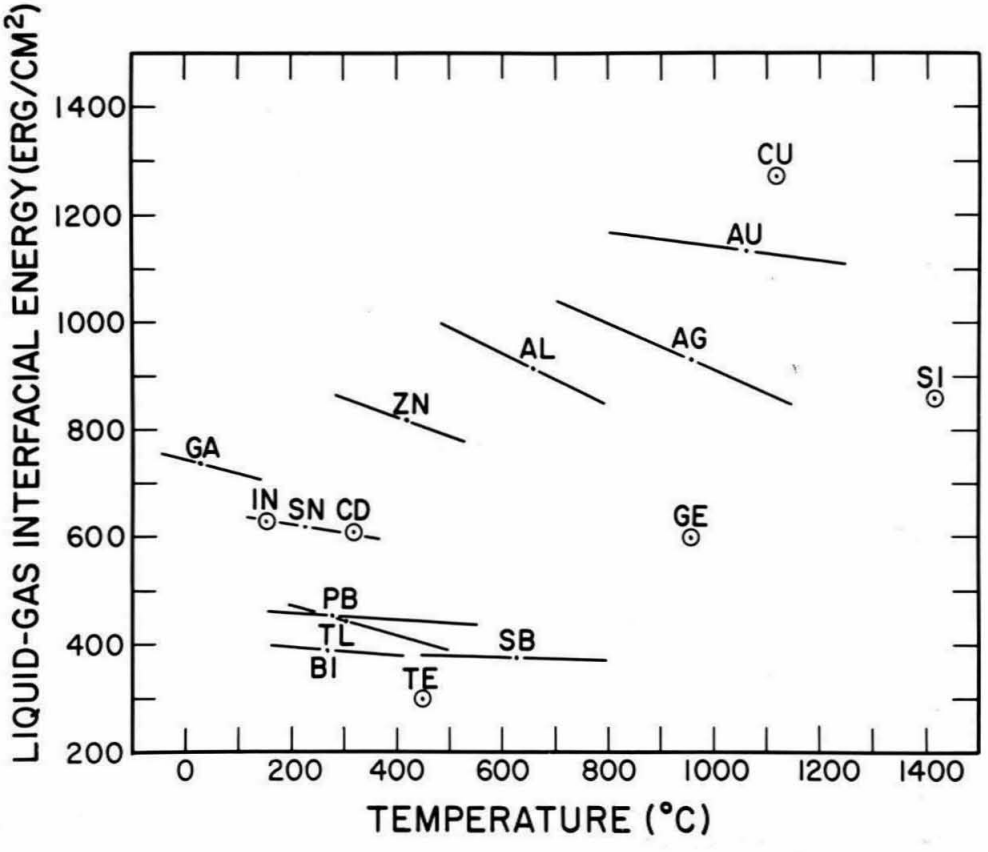

Figure 4. Liquid-gas interfacial energies, σ_{LS}, and approximate variation with temperature -- for undercooled and equilibrium liquids.

generally there is a marked decrease in surface energy if the solute has an appreciably lower σ_{LG} while only a small increase in surface energy occurs if the addition is in the opposite sense. Few data exist; deviations from this behavior may result if molecules or extensive short range order are present in the liquid. Of interest in the wetting of solids by liquids are the interfacial energies as well as the liquid-gas and solid-gas surface energies but the former are rarely known. In these circumstances, it is customary to use the necessary but not sufficient condition $\sigma_{LG} \leq \sigma_{SG}$ as a criterion for spreading. It has been noted that the contact angles for liquids advancing on solids are usually greater than those for a receding liquid and this may be related to surface roughness or surface reactions [8]. High surface energy materials are chemically reactive with absorption and/or gas reactions tending to lower the surface energy.

Because of the considerable ignorance concerning spreading phenomena, even under more or less controlled conditions, one cannot expect that much of an understanding is possible for the technique at hand and this is indeed so. There is, for instance, the possibility of a gas layer limiting heat transfer. As for the consequences of the rotating target, it is known that it is not indispensable, since some metastable structures were obtained in alloys

quenched onto stationary plates. It is believed that the primary effect of the rotating substrate was to continually present a fresh surface to the impinging droplet. That is, it is advantageous that molten material incident on the cooling surface at a given instant not be deposited on the material laid down previously. It may be argued that the centrifugal forces on the molten layer produced more intimate thermal contact with the substrate but an approximate calculation shows that the effective pressure due to rotation was only about 2 psi. The greater contribution to efficient heat transfer between molten layer and substrate was probably due to the radial component of momentum of the incident droplet. However, another compromise had to be made here since it seemed that grazing incidence favored spreading.

Since an important consideration was convenience, the surface of the substrates were prepared in ways which admitted wide variations. Copper strips, used for most of the work, were treated thus: polishing with 320 or 400 grit emery paper of the strip in the wheel rotating at a few hundred or so rpm until bright, followed by application of an acetone-soaked wiper to the rotating strip to remove the dust, etc. Because of the tenacious oxide coat, aluminum could not be dealt with this simply and etches in various nitric acid solutions were necessary. Also, both aluminum and copper strips were lightly sandblasted and used without

further treatment. Some copper strips were polished in the usual way, carefully cleaned with acetone, reduced a few mils in thickness in a rolling mill and cleaned with acetone again. These smooth strips were not satisfactory since molten droplets appeared to bounce off with only a small portion adhering.

Bailey and Watkins [8] concluded from their experiments on the spreading of solders that surface roughness is an important factor in the rate of spreading of molten metals on solids. Parker and Smoluchowski [9] studied the spreading of some molten metals on substrates which had been carefully sanded or polished in different ways and concluded that the capillarity associated with a system of fine, interlacing grooves and striations was of considerable importance in promoting rapid, effective coverage of the surface. These studies were restricted to rather slowly spreading liquid metals on clean surfaces, sans superimposed rotation, gas afterblasts, etc., but seem to agree with the present observations.

Also in reasonable qualitative agreement with existing data are observations on "spreadability" from alloy to alloy. As seen from Fig. 4, copper, gold, and silver have markedly higher liquid-gas surface energies than the other elements cited. The experience was that copper and gold spread rather poorly and thin, coherent foils were rarely obtained (however

see below for discussion of a corollary effect); silver was a borderline case while the other elements spread nicely. Addition of an element of significantly lower σ_{LG} did seem, in general, to improve the spreadability of high surface energy materials; for instance, quenched Au-Ge alloys were obtained as coherent, thin specimens, as most easily observed for foils on resin blocks (cf. II.E.).

The overall cooling rate is, of course, critically dependent upon the thickness of the molten layer initially laid down as well as upon the heat transfer to the substrate. Given in Appendix II is an idealized calculation of the cooling rate for a one-dimensional array of wall, poorly conducting layer and material of interest. Bulk thermal parameters are assumed, thicknesses of the solidified materials are obtained from experiment and the poorly conducting layer, simulating either an oxide coat or a layer of gas, is allowed to vary in thickness and thermal diffusivity. As computed in this crude way, the overall time for the process is $10^{-4\pm1}$ sec. for cooling to room temperature.

Another estimate of the times involved was obtained by considering the circumferential extent of the spreading on the inner periphery of the rotating wheel. The lengths of the specimens were, typically, $\sim$ 1 in. although much longer when the holes in the nozzle did not intersect cleanly and molten material was sprayed out and not discharged in a

coherent lump. For a motor speed of 5000 rpm, $\sim 2 \cdot 10^{-4}$ sec. would have elapsed as the molten alloy was being deposited on the target, assuming no circumferential spreading afterwards.

Thickness was measured with a micrometer for some coherent, ductile foils which were stripped off intact. For these specimens, which were among the thickest encountered, values of 15-25μ were typical for the maximum thickness. Of course, thickness ranged all the way down to nil, as was easily seen from the cast specimens. X-ray measurements (10) suggested that 5-10μ were typical for some alloys.

No systematic study was successfully made of the effects of the several variables on the resultant quenched specimens. The results of such an effort for Ag-Cu alloys are given in III.C.a. In a general way, it appeared that, the higher the initial temperature (i.e., the "superheat"), the more easily a given material spread on the substrate. This may be rationalized by the decrease in surface energy with temperature and the increased fluidity. Opposing this was the possibility that the molten layer laid down on the substrate was energetically unstable and, in an effort to reduce its surface area, attempted to clump and form "lenses." These hummocks were somewhat thicker and would not cool as rapidly. If the clumping proceeded far enough before solidification, the foil would be incoherent and discontinuous. Tendencies

like this seemed to have appeared, e.g., gold, although the phenomenon was not unquestionably isolated from the other spreading effects. The free surface of the specimens, in general, was irregular and hilly while the surface cast against the substrate faithfully reproduced the scratches and striations of the wall.

In Fig. 5 is a sketch of a typical specimen which illustrates some of the spreading effects now discussed; approximate contour lines are sketched. At what seemed to be the initial point of incidence, the material was definitely thicker and had started to cool first but probably not most rapidly because of the adjoining addition of yet more molten material as well as because of its greater thickness. Lens formation, especially in the higher energy materials, seemed to occur randomly on the surface. There were also ripples and valleys due, perhaps, to surface waves set up at impact, propagated outward and then solidified. As suggested by the contour lines, the thinnest portions seemed to be near the edges although, perhaps, not at the edge because of the pileup of material which might be expected as a consequence of the larger contact angle of advance. The portion usually taken for x-ray examination was that so marked because it was laid down at a somewhat higher temperature and could spread well, with perhaps more intimate thermal contact and possibly some lateral heat transfer to the adjacent

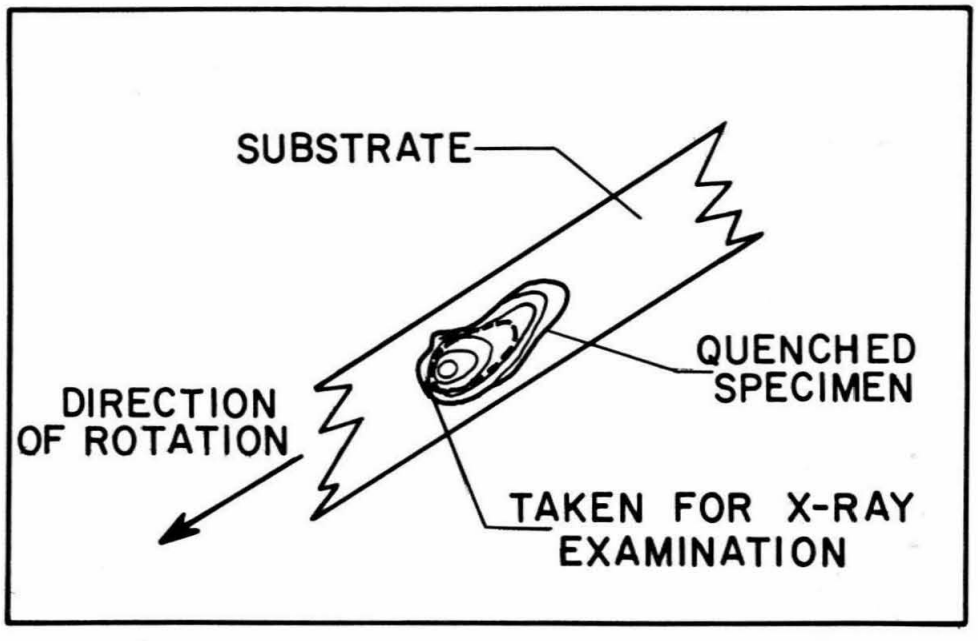

Figure 5. Sketch of specimen quenched onto substrate.

solidifying material. It is important to realize that all of these observations were made on specimens subjected to the inevitable afterblast of gas. The dotted lines indicate roughly that section of the foil which might have been ripped off by this blast, i.e., the thicker section which had been laid down first.

The factors affecting adhesion of a given solidified alloy to a given substrate are poorly understood. It is known that the surface had to be roughened or striated so that, after the flow of the melt, there was solidification with sufficient mechanical adherence to resist the blast of gas. Brittle materials, such as germanium, silicon, and some ionic salts, adhered much better to lightly sandblasted strips. There is some evidence that foils which adhered firmly to the substrate were cooled more rapidly than those which were partially or completely blown off. This criterion was used for selecting those portions of the quenched alloys which were to be examined further.

The observations and experience of Pond[4] are reviewed.

Molten alloy was supplied to a tube, one end pressurized with gas and the other terminating in an orifice through which the stream of metal was ejected onto the polished inner surface of a rotating bowl. Low melting point alloys were used with gas pressures of $\sim$ 15 psi and ejection velocities controlled in the range of a few hundred ft/sec; for appropriate geometries and target velocities, filaments of various

thicknesses were obtained in great lengths as they were thrown out of the bowl after solidification. Materials, ejected obliquely onto the cooling surface, flowed more easily with increased superheat. As target velocity was increased relative to ejection velocity, filaments became thinner, then discontinuous and, finally, were obtained only as flake or powder; conversely, for given target velocity, this sequence occurred as ejection velocity was decreased. To produce the thinnest possible filaments, it was claimed that very great superheat, minimum ejection velocity and very high surface speed were simultaneously required. The filament surface contacting the target was smooth and reproduced the chill block marks, while the other side featured ripples, valleys, etc. It was claimed that coherent filaments down to $\sim 1\mu$ thickness could be produced.

Since Pond was unaware or uninterested in the possibilities of producing metastable phases by rapidly cooling certain alloys from the melt, there is no experimental basis for comparing his cooling rates with those obtained in the present work. That is, there is the question, resolvable only by experiment, as to whether the metastable structures, such as described in this thesis, can be obtained with Pond's device.

In the meantime, other improvements have suggested themselves in the course of the present work. Reproducibility

of the shot is a desirable goal and some progress in this direction can be made, it is believed, by simplifying the geometry of the crucible as well as by carefully controlling the manifold factors -- driving gas, crucible dimensions, temperature, etc. Also bearing on this is the problem of contamination, which is ever critical for several rather reactive alloys. Such a problem can never be completely solved but the use of more nearly non-reactive crucibles, an inert atmosphere or vacuum and a crucible which can be heated more rapidly will certainly be improvements. Clean, high surface energy, yet nonreactive substrates of high thermal mass and conductivity are desirable and, for efficient spreading and adherence, a network of striations seems to be necessary. While a more powerful driving force might be of some advantage, it is of more interest to minimize the after-blast of gas. To get the target further away from the hot crucible and yet have coherent droplets impinging on the cooling surface is a problem obviously interrelated with those cited above. It is believed that a longer, more carefully finished hole would minimize the dynamic instabilities of a moving droplet. As implied in the foregoing statements and in the absence of contrary results from, say, Pond's device, it is believed that the highest cooling rates will be obtainable only with small quantities of material.

C. ALLOY PREPARATION

Alloys were usually made up in 1.5 to 5 g. quantities, with errors in the weighing-out of the components < 1.5 mg. The first melt was made under hydrogen in quartz, alumina or graphite crucibles with induction heating. The slug was remelted under argon and cast into 1 mm wires by sucking into quartz or alumina tubing (Fig. 6). From the slight weight loss incurred in the initial melt and with the assumption that similar losses occurred during casting, estimates of the precision of the alloy compositions were made; analyses of the flakes obtained after quenching were not feasible because of the minute amount of material.

Alloys were prepared in this manner only for convenience. Alloys prepared by other techniques were, of course, suitable for use in the rapid quenching apparatus with the sole criterion being homogeneity over the dimensions of the charge, typically ~ 1 mm^3.

D. X-RAY DIFFRACTION PROCEDURES

Qualitative work was done in a Norelco goniometer with large flakes pasted onto a glass slide or sample plus substrate clamped flat in specimen holders (Fig. 7). Specimens mounted on resin blocks (II. E.) were slipped into the rotary head.

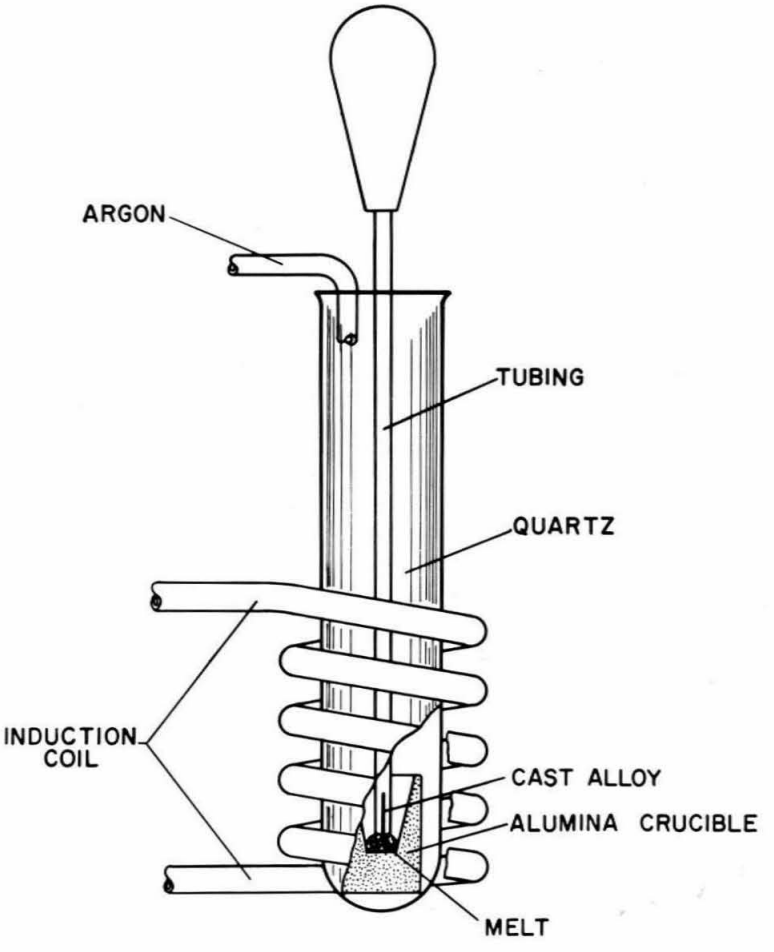

Figure 6. Casting of liquid alloys into wires.

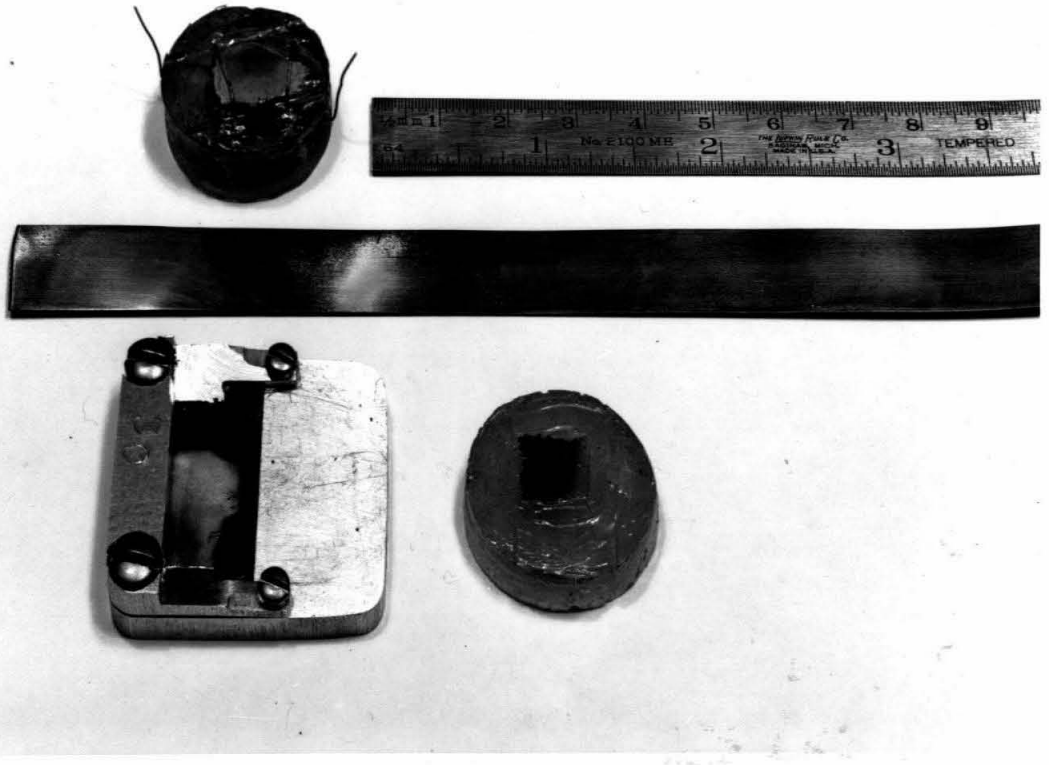

Figure 7. Specimens as quenched onto copper substrate, clamped in holder, and mounted on resin block.

Quantitative work was done with Norelco 114.6 mm diameter Debye-Scherrer cameras. Specimens were stuck onto 2-5 μ diameter quartz fibers with celvacene. Flakes > 0.3 mm^2 in area could be positioned normal to the incident beam and exposures made with the specimen stationary. Information about grain size and preferred orientations thus was often readily obtained. Most specimens were rotated during the exposure, however.

The positions of the diffraction lines on the films were located to within 0.05 mm for sharp lines; less precision was possible for broad and diffuse lines. A linear correction was applied for film shrinkage, which was less than 0.4%. Spacings were obtained and visual intensities estimated for the several reflections. For cubic structures, spacings were plotted against the Nelson-Riley function and the parameter and errors estimated from the extrapolation to $\vartheta = 90^\circ$. For hexagonal and tetragonal structures, an axial ratio was assumed and the c, a parameters calculated and plotted separately against the Nelson-Riley function. Extrapolations were made and a new axial ratio estimated, etc. until a good fit was obtained. All spacings are in Angstroms as computed relative to λ (CuKα) = 1.54178 Å, λ (CoKα) = 1.79020 Å for the unresolved lines and λ(CuKα_1) = 1.54050 Å, λ (CoKα_1) = 1.78890 for the resolved doublets. All work was done at room temperature, 26 $\pm$ 3°C.

To examine specimens at lower temperatures, a vacuum holder for the GE XRD-5 diffractometer was used (Fig. 8).

E. MISCELLANEOUS TECHNIQUES

To remove the quenched specimen more or less intact from the substrate, nucleated resin was poured into a greased teflon-lined mold (Fig. 9) and allowed to set. With the foil cast into the face of the resin block, the gross variations in thickness were evident and many areas were transparent to visible light.

For specimens cast onto blocks, the type of electrical conductivity (p or n) was determined with a thermoelectric tester[11] with copper lead wires. Resistivities were estimated with an ohmmeter. Attempts to determine the sign of the resistance change at liquid nitrogen temperatures were usually unsuccessful because of the cracking of the foil and/or resin blocks.

Specimens were given anneals and the resulting transformations followed by x-ray diffraction. Most of the samples studied were merely heated for given times at given temperatures in ovens or furnaces in air while on the copper or aluminum strips clamped in the specimen holders.

For estimates of the effects of severe deformation on the decomposition of the nonequilibrium phases, specimens quenched onto the substrates were cooled in liquid nitrogen and reduced in thickness in a rolling mill or ground to powder in a mortar.

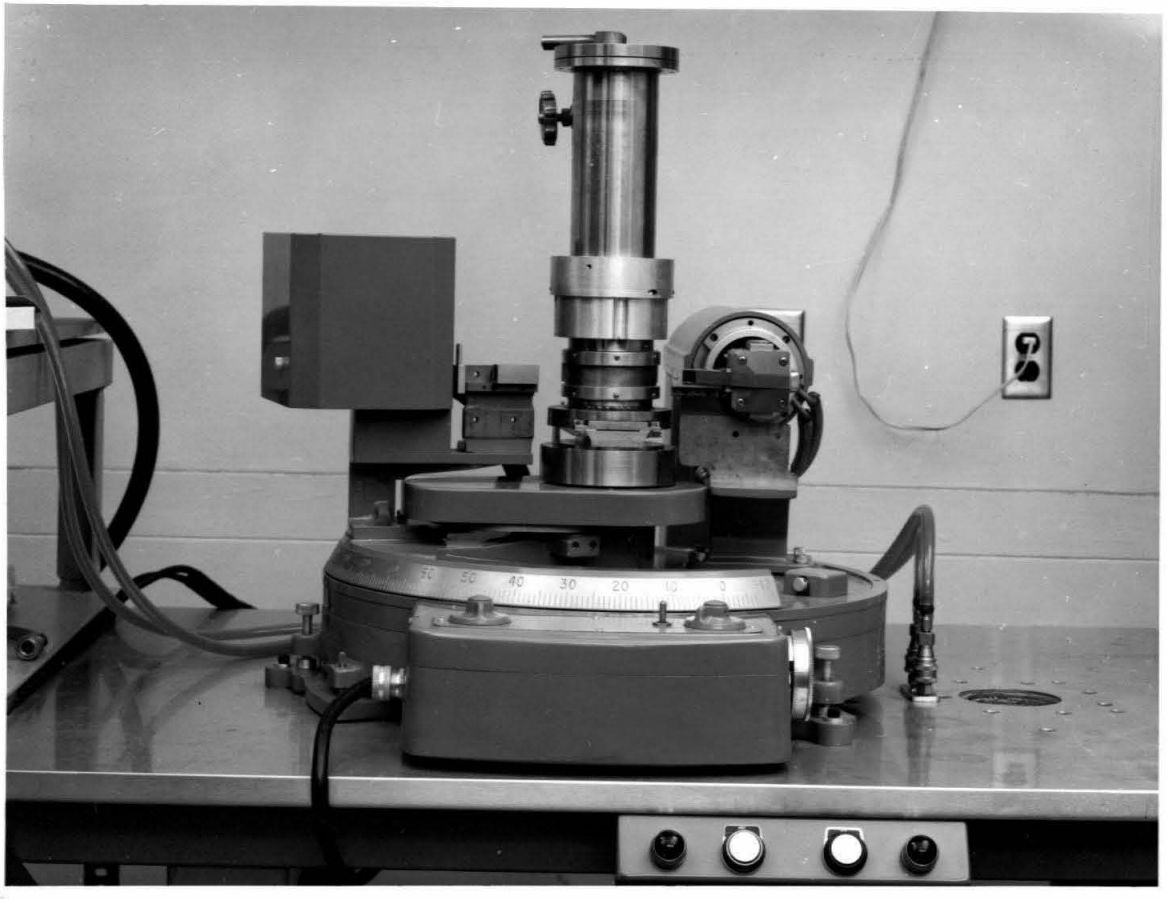

Figure 8. Low temperature vacuum holder -- "camera" -- for diffractometer.

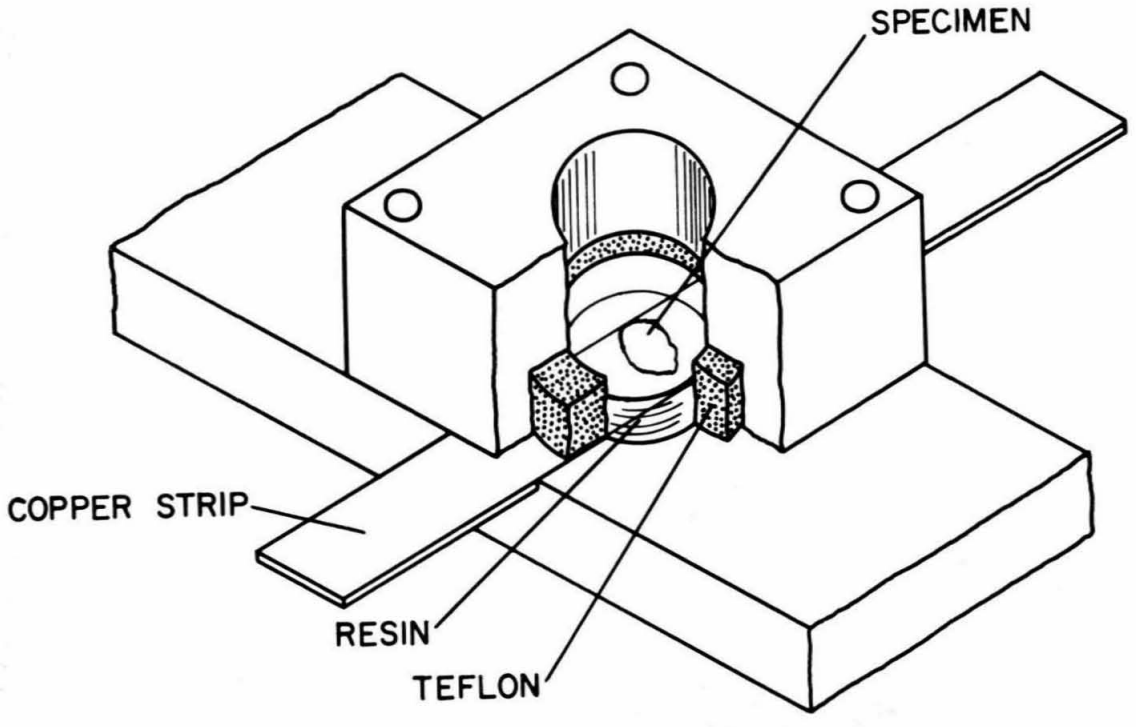

Figure 9. Cutaway view of mold for mounting quenched specimens onto resin blocks.

III. EXPERIMENTAL RESULTS

A. INTRODUCTION

The concept of equilibrium has had farreaching consequences in the physical sciences; equations of great generality are used to describe matter in the unique state of equilibrium. The understanding of nonequilibrium states, however, is at a somewhat more primitive level.

The nonequilibrium phenomena of interest in this thesis are those metastable phases and structures obtained by solidification at rather high rates of cooling. Here specific reference is to structural relations between atoms, crystalline and otherwise, as detectable by x-ray diffraction and not to the morphological macro-structural relations between grains, phases, surfaces, etc. The structures obtained with the usual cooling rates are, in general, not too different from the equilibrium structures and have usually not been systematically investigated.

In the hope of uncovering systematic relationships among the nonequilibrium phenomena, it is preferable to restrict efforts to those systems where considerable data have been accumulated for the equilibrium states. This thesis is limited to phenomena in metals and metallic alloys, ionic salts and similar high surface energy substances. A survey of the literature on nonequilibrium structures obtained upon solidification has been attempted and some of the observed

phenomena are discussed in the following.

With the knowledge from thermal analysis that solid thallium undergoes a phase change, Sekito[12] attempted to determine the crystal structure of the high temperature polymorph. Having only room temperature x-ray apparatus, he attempted to retain the high temperature form by quenching the solid from above the transformation temperature. Since the phase obtained was the usual low temperature form, hexagonal close-packed (hcp), he quenched from the liquid and found a new phase -- face centered cubic (fcc). Later work with a high temperature camera showed the high temperature polymorph to be body centered cubic (bcc), although this finding seems to be disputed also. The history is recapitulated in more detail in III.B., where the present experiments, which do not resolve the confusion, are described.

Cech[13] found that small particles of iron-nickel alloys melted and then slowly cooled in a hydrogen atmosphere solidified in the bcc structure when a fcc or tetragonal structure was expected. Further investigation showed that the bcc particles came directly from the melt and that no solid state transformations were involved. The details are given in App. I, with the results of the present work for the same alloy system. The most important conclusion was that the occurrence of the bcc phases could be related to the Fe-Ni equilibrium phase diagram.

Covington, Groenwolt and Howlett[14] have found a metastable compound upon annealing bismuth-rich Cu-Bi melts at various temperatures and cooling rather slowly until solid. Only small needles of the compound could be obtained; micro-analysis suggested a composition $\sim Cu_5Bi_2$ and the crystal structure could not be determined although it was not of cubic symmetry. No new structure was obtained by rapidly quenching 33 at.% Bi;Cu melts with the present technique. Covington, et al. suggested that a surface energy contribution to the free energy may cause the compound to become the stable phase in the absence of copper nuclei. They also commented that "a distinct flattening in the liquidus curve in the range of the probable composition of the compound suggests association in the liquid" but this is hardly the case, since such flattening infers instead imminent unmixing in the undercooled liquid. The discovery of Covington, et al. thus lacks explanation and seems to be isolated in the sense that it does not point to the way for further work.

Pawlek[15], solidifying zinc-base alloys in a device which was a forerunner of the Falkenhagen-Hofmann model (II.A.), found that several complex peritectic phases could be suppressed. Schramm[16] proposed that these solidification phenomena be interpreted in terms of a "metastable phase diagram" in which all the usual features of equilibrium phase diagrams were to be preserved in spite of the

inapplicability of Gibbs' phase rule. Such concepts have also been proposed elsewhere; viz, on rapid solidification of germanium-rich melts, the crystallization of the δ-phase ($FeGe_2$) was suppressed and a metastable eutectic, β (Fe_2Ge) + Ge, formed[17] and, also, on solidification of Cd-Sb melts, a metastable Cd_3Sb_2 phase was formed in preference to the equilibrium configuration which featured, rather, a CdSb phase[17].

Falkenhagen and Hofmann[2] carried out a somewhat systematic investigation on the extension of solid solubilities in some alloys by rapid solidification (cf. II.A.). Their results are presented in the following table:

Solvent	Solute	maximum solid solubility (at.% solute) equilibrium	rapid solidification
Al	Ti	0.09	0.19
Al	V	0.18	0.55
Al	Cr	0.45	2.85
Al	Mn	0.7	4.7
Al	Fe	0.026	0.082
Pb	Na	10.1	23.8
Pb	Te	0.16	0.32
Pb	Ca	0.52	0.95
Cu	Cr	0.9	1.8

Except for Al-Mn (cf. App. III), there was no attempt to verify or extend these results in the course of the present work. Among the interesting results of the F-H work were the measured undercoolings. For the aluminum-base alloys, undercoolings of 100°C were consistently observed, with even 200 - 300°C noted for the manganese and chromium alloys in

which the greatest increases in solid solubility were obtained. From the limited number of alloy systems studied, F-H concluded that significant extensions of solid solubility may be expected for binary systems characterized by rising liquidus curves (due generally to the occurrence of intermetallic phases with high melting points) near the solvent. They also pointed out that, for those aluminum-base alloys containing 0.1 at .% solute where the "ablosearbeit" was known; viz., Mg - 27 kcal/mole, Si-32, Cu-42, Mn-79, extended solid solubility was obtained only in the latter.

Salli has been active in this area since 1952 and two of his papers[3] [18] were available in translation. These papers are quite disconnected and verge on incoherence (due possibly to difficulties in translation), but, nonetheless, a summary of his observations is attempted. In the 1958 paper[3], it was stated that extrapolations from the equilibrium phase diagram were sometimes valid, when made in accord with the Clausius-Clapeyron equation. A consequence of the analysis was that slightly supersaturated solid solutions decompose more rapidly than more strongly supersaturated ones. It was stated that nuclei of metastable and stable phases are initially present and that "the separation...takes place, as it were, during the 'competition' of the two phase diagrams" (i.e. stable and metastable). That is, it was assumed that

the metastable situation can also be characterized by a phase diagram. At large undercoolings, it was postulated that "diffusionless" transformations occurred. From examination of successive layers of some quenched samples, it was found that, for the material directly in contact with the substrate, a supersaturated metastable solution of composition close to that of the liquid was formed; in the next layers, the usual multiphase structures, more or less, were found. It was concluded that the relative rates of growth from the undercooled liquid were most important in determining which phase, metastable or stable, predominated.

In the 1960 paper[18] by Salli and Miroshnichenko, some features of the crystallization of eutectic-type alloys were discussed. The tendency to form supersaturated primary solid solutions in systems with intermediate phases was again noted. Also mentioned was the possibility of obtaining lightly supersaturated solid solutions by "crystallization without diffusion." For the simple binary eutectic systems (without intermetallic phases) Al-Si, Pb-Sn and Bi-Sn, primary solid solutions with concentrations less than the maximum equilibrium solid solubility were found, which was related to the undercooling and indeed taken as a measure of it. Again, distinct "metastable phase diagrams" were postulated and parallels with the equilibrium phase diagrams drawn.

Little further systematic thought of value has been

found in the literature. The treatment by Jackson[19] of the kinetics of solidification was of some interest though because it claimed to describe the deviations from equilibrium for different growth rates of the solid from a melt. This exposition is based on the interfacial kinetics description[20] of the liquid-solid transformation, an approach which is considered complementary to the usual viewpoints that emphasize more heavily the nucleation processes in solidification. Foremost among the latter are the theories developed by Turnbull and coworkers[21][22] for heterogeneous and homogeneous nucleation. Although the latter seems to be in reasonably good shape, the former has been seriously challenged, especially by the experiments of Sundquist[23].

The scope of this thesis is limited to the solidification processes and matters directly related to the attainment and retention of metastable solid structures. Solid state transformations are dealt with only to the extent necessary to explain the observations and to elucidate, if possible, the solidification mechanisms. The significance of metastable solid structures thus obtained can only be given brief comment here.

B. ELEMENTS

Several experimentally convenient pure elements were quenched and the following possibilities, or some combination

thereof, existed; (i) the equilibrium crystalline structure would be obtained, (ii) a crystalline structure, stable at higher temperatures, would be retained, (iii) a non-equilibrium structure, not necessarily crystalline, would be gotten. The close-packed elements magnesium, aluminum, copper, nickel, silver and gold were quenched to room temperature from a few hundred degrees centigrade above their melting points and, as expected, only the usual crystal structures were observed. Silicon and germanium were also quenched to room temperature and only the characteristic diamond structure noted. The high temperature fcc structure was the predominant phase detected in cobalt films, although some hcp lines were detected, which was not unusual[24]. Manganese was quenched from 1300°C to room temperature. Most of the lines in the Debye-Scherrer film can be correlated to the α-Mn structure; other lines, mostly faint, probably indicated some contamination. The x-ray results for quenched iron are discussed in App. I. Quenched to liquid nitrogen temperatures, as well as to room temperature, with only the usual crystalline modifications detected, were antimony, zinc, cadmium, bismuth, lead, mercury, and indium. In tin, the body centered tetragonal structure was retained because of sluggishness of transformation to diamond structure[25].

Thallium was investigated more intensively than the above mentioned elements because of the considerable confusion

concerning the crystal structures. Sekito[15], working in 1930 when neither the crystal structures of the high temperature form (stable from 230°C to 303°C, the melting point) nor the low temperature form (stable below 230°C) were known with certainty, undertook to determine these structures. The low temperature form was found to be hcp and this has been verified by Lipson and Stokes[26]. Because his x-ray equipment was limited to room temperature operation, Sekito attempted to retain the high temperature phase by quenching into ice water, with specimens coated with glycerol to avoid oxidation. It was not possible to obtain anything but the hcp phase by quenching the solid from above 230°C. By quenching the liquid, a fcc phase was obtained if the water-tank was not too shallow or the quantity of metal not too great, (say, not more than 5 g). Under these latter conditions, which imply too low a cooling rate, the hcp modification was formed. Sekito then concluded that the high temperature phase was fcc. Lipson and Stokes[26], working with a high-temperature camera, found that the structure at 262°C was bcc although some hcp lines were noted. The purity of their thallium was >99.995% while Sekito did not state the purity of his material. Schneider and Heymer[27] determined the lattice spacings of thallium at temperatures within the field of the high temperature polymorph and found the structure to be fcc, as Sekito had suggested but in

contrast to the results of Lipson and Stokes.

In view of this unsatisfactory situation, an attempt was made to reproduce the face centered cubic structure of Sekito with the present technique, which is capable of much greater cooling rates. Thallium of purity $> 99.99\%$ was quenched from various temperatures onto copper and aluminum at room and liquid nitrogen temperatures. Only the hcp structure was ever observed.

C. ALLOYS

From equilibrium phase diagrams, working hypotheses were developed to predict the occurrence of some metastable structures in alloys rapidly quenched from the melt. Some of these working hypotheses are now described, followed by a presentation of the experimental results and the attempts to develop adequate criteria.

Chemically similar components possessing the same or similar crystal structures generally form complete solid solutions when they are not too grossly different in volume/atom. As the differences become greater, it is generally found that eutectic systems with limited solid solubilities and then monotectic systems with very limited solid solubilities and some liquid immiscibility occur. It was initially expected that metastable solid solutions might be obtained, for these alloys, by quenching from a region of liquid miscibility. Metastable solid solutions have

indeed been found for the eutectic system Ag-Cu, in which the components crystallize in the fcc structure, and also for the pseudo-binary eutectic system GaSb-Ge, in which the components crystallize in the closely related zincblende and diamond structures respectively, but not for the eutectic system Cd-Zn, in which each component crystallizes in distorted hcp structures with similar axial ratios. For the relatively well-studied Ag-Cu and Cd-Zn alloy systems, the available data are examined for clues to this diametrically opposite behavior, which was not expected from an elementary consideration of the phase diagrams.

For metals and intermetallic phases, it was expected that the solid solubilities might be extended beyond those found at equilibrium, regardless of the crystal structures of the components. For this very large class of problems, no systematic results have emerged in the course of the present work. However, for some silver-base alloys of considerable theoretical interest, lattice parameter measurements of multiphase quenched alloys suggest metastable extended solubilities.

It was also expected that new structures, hitherto unknown in the particular alloy system, could be obtained. These new structures might be merely the suppression of a complicated equilibrium phase; they also should not be restricted to being crystalline, although noncrystalline

solid structures are not found in bulk metallic systems. Discussed in this thesis are the metastable hcp structures obtained in Ag-Ge alloys.

a. Solid solutions among components of similar crystal structure.

1. Ag-Cu

Silver and copper are similar chemically and structurally, both crystallizing in fcc lattices. The simple eutectic alloy system has been widely studied and there is good agreement on the equilibrium phase diagram[17] (Fig. 10). Pertinent experimental and theoretical information is discussed, especially in conjunction with the Cd-Zn alloy system, after presentation of the present experimental results.

Alloys were prepared in quartz crucibles from elements of purity $>$ 99.9%. The alloys were usually quenched onto copper from graphite nozzles heated to $\sim$1300°C although different temperatures, substrates, etc. were also used. From many films, estimates of the lattice parameters of the metastable solid solutions obtained were made and are presented below; also given there are the estimated accuracies of the alloy compositions and the characters of the other phases detected.

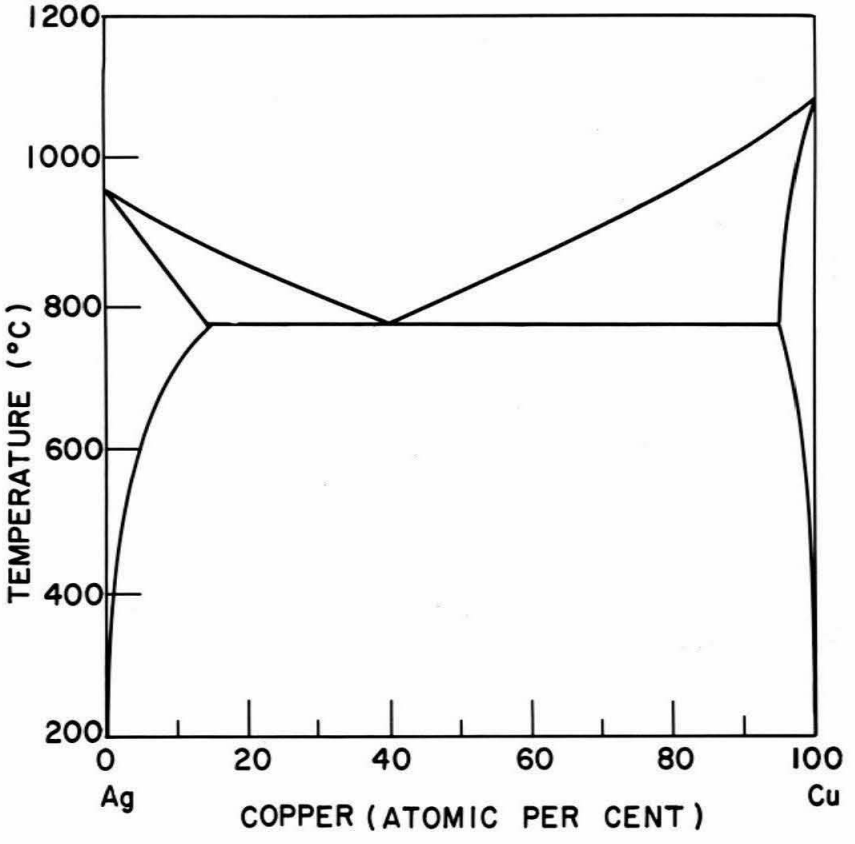

Figure 10. Equilibrium phase diagram of Ag-Cu system.

Alloy (at.%Ag)	a(Å)	Comments
0	3.6153±3	
11.5±0.2	3.6860±10	
25.0±0.4	3.759±3	faint silver-rich phase detected, high angle lines unresolved.
37.1±0.2	3.8164±10	faint silver-rich phase detected
50.0±0.3	3.8815±20	faint copper-rich phase detected
60.0±0.3	3.9250±15	faint silver-rich phase detected
70.0±0.2	3.9686±10	faint copper-rich phase detected
77.0±0.3	3.9980±15	
100	4.0853±3	

Grain sizes were estimated as $\sim 1\mu$ from the broadening of the diffraction lines. Films of stationary specimens did not suggest any preferred orientations.

It is to be emphasized that the results tabulated above represent the best of much work; the faint, nearly equilibrium phases just could not be suppressed in the indicated alloys, at least not to a level below that detectable by the present techniques. In this respect, the lesser scattering power of copper may allow it to go undetected relative to the same amount of silver with a few percent as the approximate threshold of detection here. The presence of the other phases may be rationalized in terms of the competitive growth

or precipitation processes (III.D.), but also may be due to other factors more nearly within control of the investigator. For instance, hesitation in pulling the rotating wheel away from the hot nozzle after a shot may result in some annealing out of the metastable solid solutions. Mechanical working during the removal of the specimen from the substrate may also result in decomposition. The possibility exists that certain areas have cooled at much lower rates than adjacent material and hence are not essentially all metastable solid solution; indiscriminate choices of the specimens to be further examined would then result in detection of the nearly equilibrium phases. Attention was paid to these possibilities here insofar as was possible.

Considerable effort was expended with these alloys in an attempt to separate the effects of the sundry variables involved in the quenching technique. This approach was far from successful, although some tentative conclusions were possible. Used as a qualitative indicator were the relative intensities of the metastable and nearly equilibrium phases, under the plausible assumption that the conditions under which a good deal of the nearly equilibrium phases formed were somewhat less stringent. Copper substrates, treated in the usual way (II.B.c.), seemed to be somewhat better than the other materials, although the latter were occasionally adequate. The pressures of the driving gases in both Model I

and II were varied over a few hundred psi without significant differences. As expected, alloys in this system quenched from graphite nozzles and alumina inserts were much alike. Contamination seemed to be unimportant except for the occasional oxidation noted for some of the copper-rich alloys. Experiments with different wheel speeds were inconclusive and, occasionally, metastable solid solutions were achieved even with a stationary wheel. By following the surface temperature of the nozzle with an optical pyrometer, it was found that nearly single-phase solid solutions could often be obtained at superheats of as little as 25-50°C.

It was also of interest to test the possibilities of quenching these alloys into liquids. To this end, a charge of the 60 at.% Ag;Cu alloy was fired from a graphite nozzle at 1300°C into a 10 mol.% NaOH;H_2O solution which had been chilled with ice. The molten projectile easily penetrated the Saran wrap holding back the inclined coolant and then disintegrated into many spherical particles of a few μ diam. Only the copper- and silver-rich phases were detected in these particles.

2. Cd-Zn

Cadmium and zinc are very similar chemically and crystallize in distorted hcp structures of similar axial ratio. The equilibrium phase diagram of the binary alloy system[17]

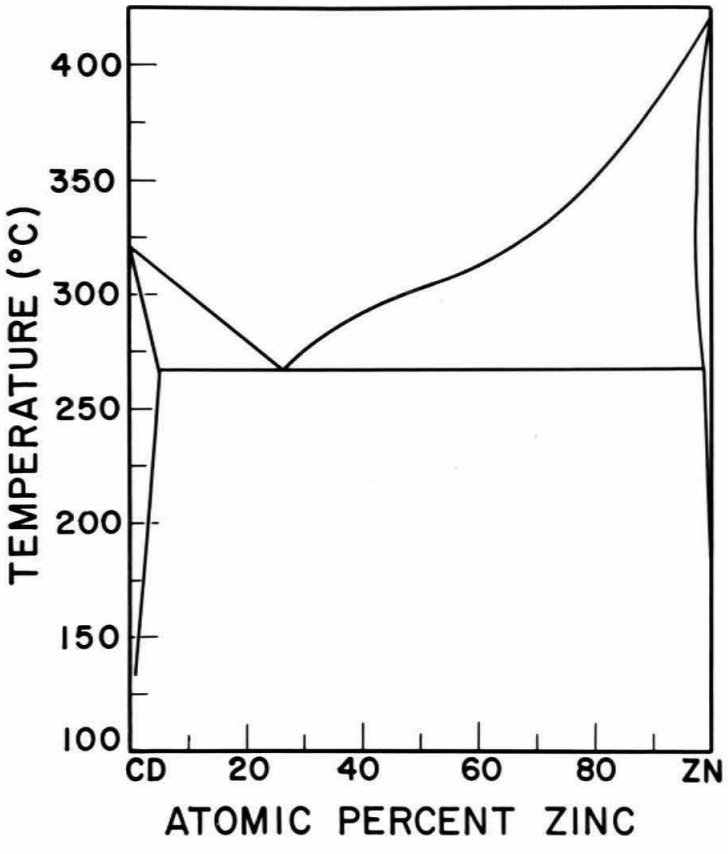

Figure 11. Equilibrium phase diagram of Cd-Zn system.

(Figure 11) is well determined.

Prepared in quartz crucibles, with no apparent segregation, were the following alloys: 15, 27, 50, 75 and 85 at.% Zn;Cd. Shots were made from graphite nozzles heated to 500°C and higher (despite volatilization) onto copper at room temperature and aluminum at liquid nitrogen temperature. Debye-Scherrer films of quenched alloys indicated two phases in all cases; lattice parameters were not computed because of the view that only negligible extension of the equilibrium solid solubilities had been obtained. In the low temperature camera, the diffraction peaks were rather broad and diffuse and only the strong low angle lines could be unambiguously separated from the background. There was no evidence that metastable solid solutions were obtained for the quenched alloys investigated at low temperatures.

3. GaSb-Ge and other materials

The work done by the present investigator and previously reported (below) is yet valid and no emendations are necessary. Because of the lack of other experimental data for this alloy system, no further analysis is attempted.

Metastable Solid Solutions in the Gallium Antimonide-Germanium Pseudobinary System*

POL DUWEZ, R. H. WILLENS, AND W. KLEMENT, JR.
Division of Engineering, California Institute of Technology, Pasadena, California
(Received April 14, 1960)

THERE seems to be a dearth of published work on the Ga-Sb-Ge ternary system despite the great interest in the semiconductors GaSb and Ge. However, unpublished work[1] indicates that gallium antimonide and germanium may be regarded as the components of a simple eutectic pseudobinary system. The eutectic is estimated to occur at 35±10 at. % germanium at a temperature of 648±4°C. The maximum solubility of germanium in gallium antimonide is probably less than 2 at. % under equilibrium conditions.

The procedure by which small amounts of liquid alloys can be quenched rapidly enough to forestall the normal nucleation and growth processes has been previously reported.[2] A series of alloys was prepared from stoichiometric gallium antimonide ($a=6.097$ A) and zone refined germanium ($a=5.658$ A). The alloys were cooled rapidly and their resultant structures studied by means of x-ray diffraction. A single phase—with the disordered zincblende structure—was observed in all of the alloys investigated. The plot of lattice parameter vs composition (Fig. 1)[3] does not indicate significant or systematic deviation from Vegard's law.

These results were not unexpected. The zincblende structure of gallium antimonide and the diamond structure of germanium are both based upon the necessity of each atom having four nearest neighbors which, in turn, is demanded by the covalent bonding. If the conventional valancies are assigned to the elements, the number of valence electrons/atom remains four throughout the pseudobinary system. Furthermore, the germanium atoms seem to be of such a size as to fit substitutionally into the lattice without causing undue distortion. From a qualitative study of the intensities of the diffraction lines on the Debye-Scherrer films and the absence of any detectable splitting of these lines, it is hypothesized that germanium substitutes randomly in the lattice, and does not destroy the cubic symmetry.

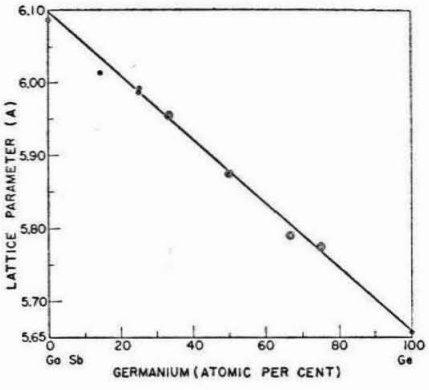

FIG. 1. Lattice parameter vs composition in the germanium-gallium antimonide psuedobinary system.

Acknowledgments are made to J. O. McCaldin for providing the alloys and for his continuing interest in this investigation.

* This work was jointly sponsored by the U. S. Office of Naval Research and the U. S. Atomic Energy Commission.
[1] J. O. McCaldin (private communication).
[2] Pol Duwez, R. H. Willens, and W. Klement, Jr., J. Appl. Phys. 31, 1136 (1960).
[3] The graph of Fig. 1 is based on the nominal composition of the alloys before melting. It has not been possible to obtain reliable chemical analyses thus far. Maximum deviation between nominal and actual compositions might be as large as 5 at.% germanium.

Perhaps the most important consequence of this work is that the rapid quenching technique is also applicable to covalently-bound materials. There is no a priori reason why metastable solid solutions between appropriate ionic salts should not be obtained with this technique although no positive results were obtained in a series of experiments.

b. Solid solutions in silver-base alloys

In the work on Ag-Ge alloys (III.C.c.), it was discovered that the lattice spacings of the metastable fcc structures

appeared to increase linearly with germanium content up to 13.0±1.0 at.% Ge. Despite the inability, in general, to obtain single-phase alloys, it was suggested that the primary solid solubility had been extended beyond the maximum equilibrium value of 9.6 at.% Ge. According to the viewpoint of Hume-Rothery, et al.[28], the equilibrium solid solubility of germanium in silver is "restricted"; however, the metastable solubility limit corresponds to an electron concentration of 1.39±3 -- a value given considerable empirical support. Other similar silver-base alloys, with restricted solubility limits, were then investigated in order to determine the metastable primary solid solubilities attainable with the present technique.

The experimental procedures and results for Ag-Ge alloys are presented in III.C.c. Similar methods were employed for the antimony, bismuth, lead, tin and silicon alloys except, for the latter, it was necessary to melt in alumina crucibles as well as to use alumina inserts in the graphite nozzles. To minimize volatilization, the antimony, lead and bismuth alloys were quenched from 1200°C. All elements were of purity $>$ 99.9%. Compositions were believed accurate to ±0.1 or 0.2 at.% for the tin and antimony alloys; compositions for the other alloys are only nominal.

Some equilibrium data on the silver-base alloys of interest are given in the following table:

Solute	Maximum equilibrium solid solubility[17]		Comments[17]
	at.% solute	electron concentration	
Ge	9.6	1.29	simple eutectic system
Si	? small	?	simple eutectic
Sn	11.5±0.2	1.345±6	intermediate phases
Sb	7.2	1.29	intermediate phases
Bi	2.7	1.11	simple eutectic
Pb	2.8	1.08	simple eutectic

Despite much effort with the Ag-Si alloys, it has not been possible to obtain lattice spacings which are sufficiently critical to establish either the variation of lattice spacing with silicon content or the limits of solid solubility. The Si (111) diffraction line was not detected in any alloy containing less than 16 at.% Si. For alloys in the range 10-25 at.% Si, faint low angle lines were detected which could be indexed as the (10.0), (00.2) and (10.1) reflections of an hcp structure with a = 2.875±25 Å, c = 4.520±30Å, c/a = 1.572±20. In contrast to Ag-Ge, there was no range in which the hcp phase predominated at room temperature. The 16 at.% Si alloy was quenched to and examined at liquid nitrogen temperatures but no predominant hcp phase was found.

The Ag-Bi and Ag-Pb systems[17] are quite similar in that the eutectic compositions are at ~5 at.% Ag and the maximum solid solubilities in silver occur above the eutectic temperatures. For electrodeposited alloys, ~4 at.% Pb can be held in supersaturated solid solution[29]. Lattice spacings from the literature[30] [31] [32] and from the present work are plotted against Bi, Pb content in Figure 12. Metastable solubilities have been estimated from the extrapolations of straight lines fitted to the equilibrium data. Single-phase alloys could not be obtained; faint lines corresponding to the Bi(102) and Pb(111) reflections, respectively, were detected. High angle diffraction lines were invariably diffuse. No crystal structure other than those present at equilibrium was found although the hcp structure discovered by Heidenreich[33] was searched for in many quenched Ag-Pb alloys, including some rich in lead. Thus, the limits of metastable solid solubility under these conditions appear to be ~4 at .% Pb and ~ 4.5 at.% Bi.

The silver-rich ends of the Sb, Sn systems[17] are quantitatively quite similar when the phase boundaries are plotted on a temperature vs electron concentration diagram. Narrow two-phase regions separate the fcc phases from the ζ-phases, which are hcp with nearly ideal axial ratios[24] at the solubility limits. Lattice spacings of fcc structures in the equilibrium region[34] are plotted in Figure 13 with

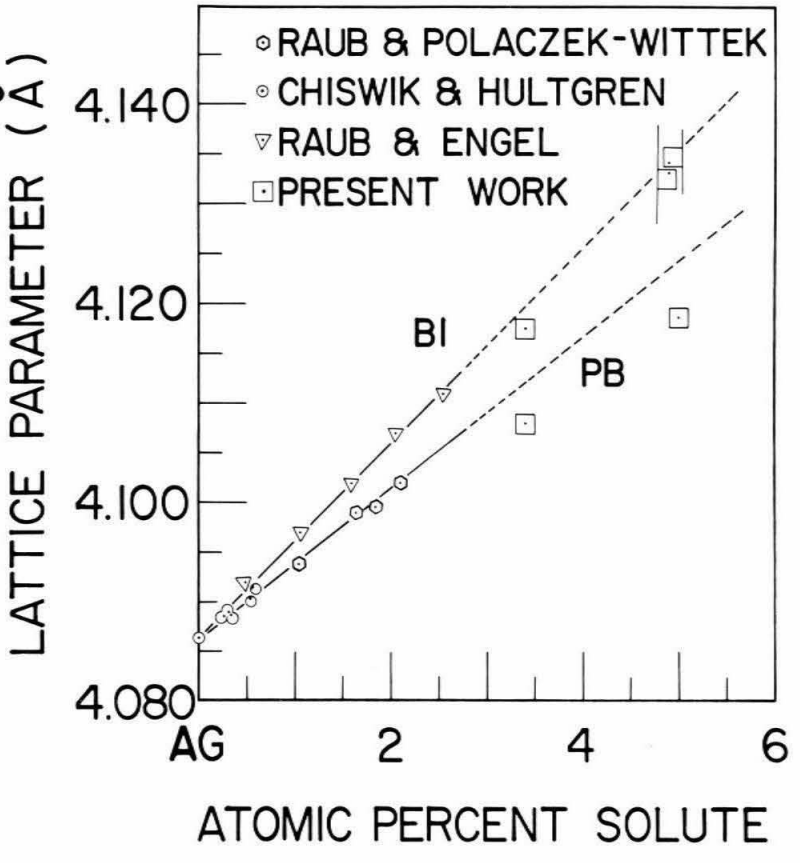

Figure 12. Lattice parameters plotted against solute concentration for face centered cubic solid solutions of bismuth and lead in silver.

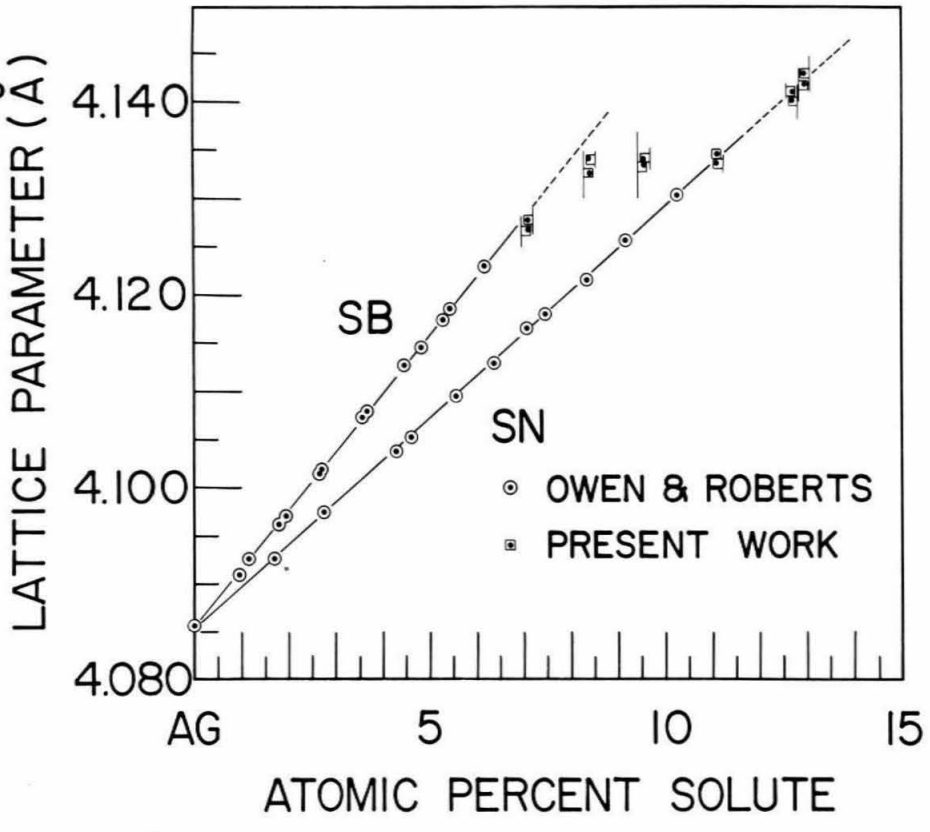

Figure 13. Lattice parameters plotted against solute concentration for face centered cubic solid solutions of tin and antimony in silver.

the present results. Hcp diffraction lines were detected in the 11.1, 12.7 and 12.9_5 at.% Sn and 7.1, 8.4 and 9.5_5 at.% Sb alloys; their relative intensity increased with higher solute content. The metastable solubility limits appear to be $\sim$ 8 at.% Sb and $\sim$ 13 at.% Sn.

Assuming that the measured lattice spacings correspond to supersaturated solid solutions, the metastable solid solubility limits for the silver-base alloys are (in terms of electron concentration); Ge, 1.39$\pm$3; Sb, 1.32; Sn, 1.39; Bi, 1.18; Pb, 1.12.

For the Ag-Sn and Ag-Sb alloys, the viewpoint taken is that the free energies of the fcc and hcp phases are nearly the same as are the nucleation and growth rates upon solidification. Thus the admixture of these phases in the quenched alloys reflects the competition between these structures which, within certain limits, are of nearly the same composition. Similarly, the metastable hcp structures in Ag-Ge alloys have free energies, etc. close to that of the fcc structures. These matters are dealt with more fully in III.D.

The Ag-Bi and Ag-Pb alloys seem to require different interpretation. As noted for apparently the first time from a survey of published equilibrium phase diagrams[17], retrograde solid solubility generally occurs in binary metallic alloys whose components are markedly different in size with the larger element as solute. This retrograde solid

solubility is usually accompanied by a flattening in the liquidus curve and, often, some immiscibility in the liquid. Such flattening presages unmixing in the undercooled liquid. Pronounced flattening in the liquidi of the Ag-Bi and Ag-Pb alloy systems are found[17] and the expected separation or tendency thereto in the undercooled liquid is suggested as the reason that the solid solubilities cannot be appreciably extended with the present technique.

c. Metastable hcp structures in Ag-Ge.

Nonequilibrium hcp structures have been obtained in Ag-Ge alloys quenched with the present technique. The experimental procedures and results are adequately presented in the following reprint.

Lattice Parameters of the Metastable Close-Packed Structures in Silver–Germanium Alloys

By W. Klement, Jr., B.S.

The lattice spacings of the metastable face-centred cubic and hexagonal close-packed phases in the silver–germanium system have been determined for alloys of various compositions which have been quenched rapidly from the melt. The quenching and X-ray diffraction techniques are discussed in detail. Results of some cold-working and annealing experiments with the quenched alloys are presented. Difficulties—both experimental and of interpretation—are briefly noted.

The lattice parameters of the recently discovered[1] *non-equilibrium* hexagonal close-packed (h.c.p.) phase in silver–germanium alloys have been obtained by means of the Debye–Scherrer technique. Similar measurements imply that the solid solubility of germanium in the face-centred cubic (f.c.c.) silver lattice is extended beyond the reported equilibrium value.

At equilibrium, silver and germanium form a simple eutectic system.[2] The limit of solubility is 9·6%[3] germanium,* and is to be considered as restricted,[4] since it corresponds to a value of $e/a = 1{\cdot}29$, where e/a, the electron concentration, is defined as the ratio of all valence electrons to the number of atoms.

This investigation was undertaken with a view to determining the properties of the metastable structures so as to provide information which may eventually lead to a clearer understanding both of the metastable structures in this system and of the equilibrium close-packed phases in allied systems such as silver–tin, silver–antimony, and copper–germanium.

Experimental Procedure

Alloys were prepared from chemically pure silver (ca. 99·95% pure) and zone-refined single-crystal germanium (⩾99·999% pure). Weighed quantities of the elements were melted by induction heating in a quartz crucible under hydrogen. The alloys were then reweighed. The estimated compositions (accurate to better than ±0·1 at.-% Ge) are given in Table I. The alloys, remelted in the quartz crucible under argon, were cast by sucking the liquid up into preheated 1-mm-inside-dia. quartz tubing and immediately quenching

TABLE I

Diffraction Intensities of Phases in Quenched Alloys

Alloy Composition, at.-% Ge	f.c.c.	h.c.p. h.c.p.′	Ge	*d*-spacings, intensities of unidentified lines, Å
9·0	s	...	...	...
9·6	s	tr	...	...
10·3	s	tr	...	...
11·9	s	tr	...	...
13·4	s	w	...	...
15·0	m	s	...	...
16·8	w	s	tr	4·10 vw
18·1	w	s	...	...
19·9	tr	s	...	...
21·6	...	s	tr	...
23·2	...	s	tr	3·76 vw, 4·14 vw
25·9	...	s	w	3·75 w, 4·13 m

s = strong, m = medium, w = weak, v = very, tr = trace.

Paper No. 2089. Manuscript received 14 February 1961. Mr. Klement is in the Division of Engineering, California Institute of Technology, Pasadena, Cal., U.S.A.

* Compositions are expressed in atomic per cent.

into water. Because of the stirring action of the eddy currents and the speed of the quench, the cast alloys were of homogeneous composition throughout. (This conclusion was verified by noting that the data obtained from different portions of a given casting were reproducible, within experimental error.) Finally, the quartz tubing was broken away and the alloy, in the form of short lengths of 1-mm-outside-dia. wire, was ready for use in the rapid-quenching apparatus.

The principles of this rapid-quenching technique have been described elsewhere.[5] Graphite nozzles (i.e. crucibles) were used in air throughout the investigation. Reactions with carbon, oxygen, and nitrogen should be negligible in the temperature range involved; also, the vapour pressures of the elements should be so low as to be safely neglected. To obtain a suitable specimen, approximately 25 mg of the alloy was loaded into the nozzle, which was then heated to 1300 $\pm$ 25° C by means of eddy currents. The molten alloy was ejected on to a polished copper strip held on the inner periphery of a rotating wheel. Heat was extracted very rapidly from the alloy, assisted, in part, by the centrifugal forces on the droplet which ensured good thermal contact with the substrate. The time necessary for the alloy to reach the temperature of the copper conductor is estimated to be a few milliseconds. (A lower limit for this time may be estimated by noting the speed of the wheel and the extent of the spreading along the circumference; this lower limit is about a half-millisecond.) The thickness of the specimen was 15 $\pm$ 5 μ.

A flake (ca. 0·7 $\pm$ 3 mm²) was carefully removed from the substrate, stuck on to a quartz fibre with Celvacene, and mounted in a Norelco Debye–Scherrer camera (radius = 5·73 cm) so that the incoming beam of filtered CuK radiation was normal to the plane of the specimen. Exposures were made for a few specimens both rotated and stationary; comparison indicated only a negligible difference in d-spacings, while the latter technique often yielded sharper lines as well as very faint lines otherwise absent on the film obtained from the rotated specimen. Thus, the procedure of not rotating the specimen was adopted. Typical exposures were for 3 h at 35 kV and 15 m.amp, using Kodak No-Screen film.

The lines on the Debye–Scherrer films were, in all cases, continuous and of uniform intensity. This indicates that there is no obvious preferred orientation and that the crystallite size is less than, say, a few microns. Broadening of the lines was noted but was not considered to be pronounced. Further investigation (to estimate the minimum crystallite size) did not seem to be justified, since the effects of residual strain (and possible stacking faults) must also somehow be taken into consideration. In this connection, it was observed that, at high angles, the K_α doublet was resolved in the predominantly f.c.c. alloys but not in the predominantly h.c.p. alloys. Consequently, the uncertainty in the determination of the lattice spacings of the h.c.p. structures was much greater than that of the f.c.c. spacings.

The positions of the sharp diffraction lines were read to within 0·005 cm; when diffuse high-angle lines were encountered, the films were reread a number of times to obtain good averaging. Corrections were made for film shrinkage. Extrapolations to $\theta = 90°$ by means of the Nelson–Riley function yielded the lattice spacings of the f.c.c. and h.c.p. structures. For the latter, various values of the axial ratio were assumed until the best extrapolated values of c and a could be obtained. Errors were estimated from the extrapolations. All spacings are given in Ångstroms with $\lambda(\mathrm{Cu}K_{\alpha 1}) = 1{\cdot}54050$ Å.

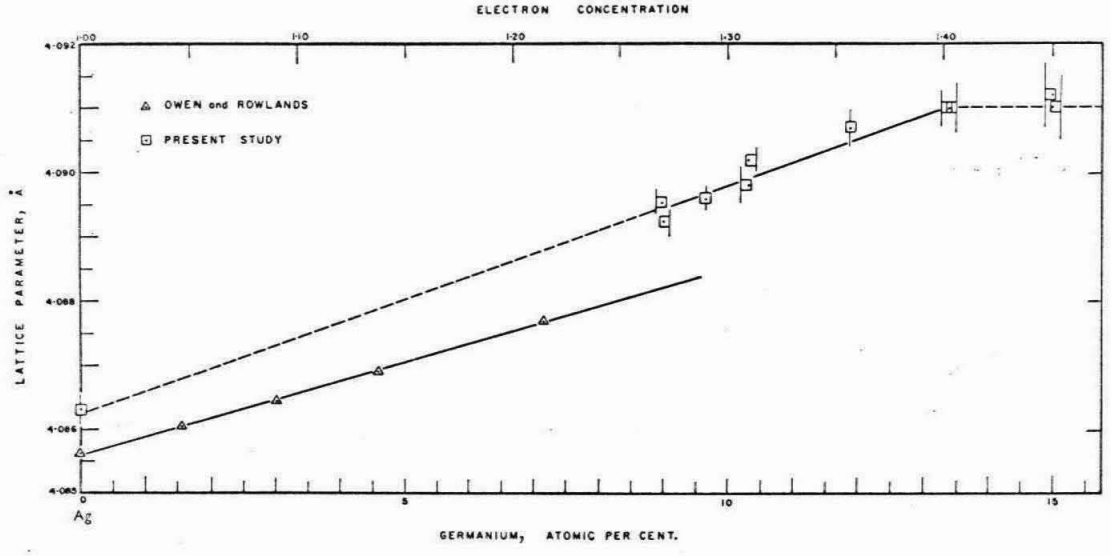

Fig. 1 Lattice parameters of f.c.c. structures plotted against composition. Uncertainties in the spacings are indicated by the vertical lines on the squares enclosing the points obtained by the best extrapolations against the Nelson–Riley function. The two sets of data were recorded at different temperatures (see text).

Results

By visual comparison of the intensities of the strong low-angle lines, e.g. the h.c.p. (10.0) and (10.1), f.c.c. (200), and Ge (111), rough estimates were made of the quantity of each phase present in the quenched alloys (Table I). Also included are the d-spacings and intensities of the several unidentified lines. The accuracy of these spacings is, of course, limited by the difficulties inherent in reading faint or diffuse lines.

The lattice spacings of the f.c.c. alloys are plotted against germanium content in Fig. 1. (In anticipation of its possible pertinence, an electron-concentration scale has been included.)

The results of Owen and Rowlands[3] are also presented, after conversion from kX to Å units. Since their work was done at 18° C (cf. 26 ± 4° C in the present work), a correction must be applied for the temperature difference.

The lattice parameters and axial ratios of the h.c.p. alloys are plotted against germanium content and electron concentration in Fig. 2. Within experimental error, the h.c.p. structure (denoted h.c.p.′) found in alloys containing ≳22–23% germanium seems to be invariant with composition. The lattice spacings of the h.c.p.′ structure in a quenched alloy containing 49·7% germanium are: $a = 2{\cdot}898 \pm 3$ Å, $c = 4{\cdot}723 \pm 3$ Å, $c/a = 1{\cdot}630 \pm 3$. Lines at $d = 4{\cdot}14$ Å (mw) and 3·72 Å (vvw) were also observed.

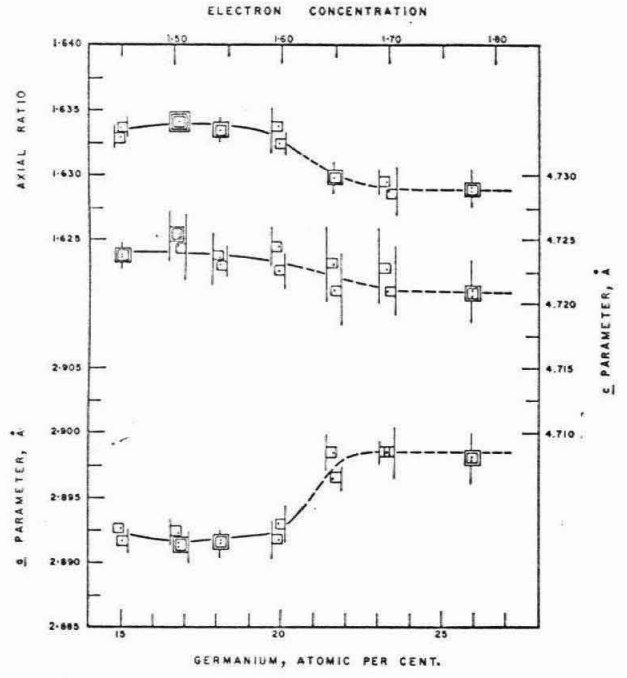

Fig. 2 Lattice parameters of h.c.p., h.c.p.′ structures plotted against composition. The meaning of the vertical lines, squares, and enclosed points is the same as in Fig. 1; for a given composition, points enclosed by squares with vertical lines on the right (or left) are obtained from the same specimen. For similar values of the spacings, the number of squares about the points denotes the number of independent data considered. In the absence of vertical lines, uncertainties in the parameters are indicated by the size of the squares. The relatively large errors are discussed in the text.

Typical intensities for the diffraction lines of the h.c.p., h.c.p.′ structures are given as a function of germanium content in Table II for the alloys of Table I ranging from 16·8 to 23·2% germanium. These may be useful for qualitative comparisons, but should not be incautiously considered as absolute measurements. Changes in the intensities, plus the appearance of the extra low-angle lines, leads to the distinction between the h.c.p. and the h.c.p.′ phases.

Other Observations

Some work was done with the h.c.p.′ phase in the 25·9% germanium alloy to obtain semi-quantitative estimates of the effects of temperature and mechanical working upon the transformation (i.e. decomposition) to the equilibrium phases.

Specimens of this alloy were quenched upon copper strips in the usual way so as to produce the metastable phase. With a Norelco diffractometer, continuous scans were taken over the angular region containing the strongest lines. Then the specimens were isothermally annealed in air until a given stage of decomposition was attained (Fig. 3). Typical times

TABLE II

Variation of Intensities of H.C.P., H.C.P.′ Diffraction Lines with Germanium Content

Indices	Germanium, at.-%						
(hk.l)	17	18	19	20	21	22	23
(10.0)	.ms			s			vs
(00.2) *	.vvs						vs
(10.1)	.s diff						vvs
(10.2)	(absent)	vw diff		ms			s
(11.0) *	.s						s
(10.3)	(absent)	vw diff		ms			s
(20.0)	.vw						vw
(11.2) *	.ms						ms
(20.1)	.m						m
(00.4)	.w						w
(20.2)	(absent)			vw			w
(10.4)	(absent)			vw			w
(20.3)		vw diff		m			m
(12.0)		vw		w			w
(12.1)	.m						m
(11.4) *	.m						m
(10.5)		vw diff		m			m
(20.4)	.(absent)			vw			vw
(30.0) *	.mw diff						mw diff
(12.3)		w diff		ms diff			ms diff
(00.6) *	.m diff						m diff

The position of a symbol (e.g. vw diff) along a horizontal corresponds to the alloy whose composition is given directly above. Continuous variation of intensity from alloy to alloy is to be inferred from the connecting series of dots; abrupt changes are emphasized by absence of dots. For alloys containing the h.c.p.′ phase (high Ge content) there is little variation in relative intensity; for alloys of somewhat lower Ge content the intensities are altered by the overlapping f.c.c. reflections (marked by an asterisk).

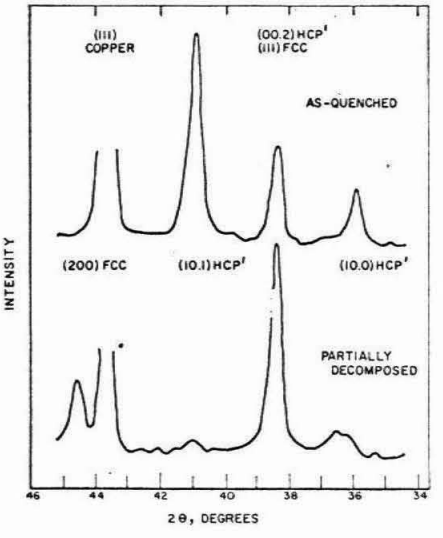

Fig. 3 Diffractometer traces of the angular region containing the strong low-angle diffraction peaks of the f.c.c. and h.c.p.′ structures. The upper trace is that of the 25·9% germanium alloy shortly after quenching; the lower trace represents that degree of decomposition referred to in the isothermal-annealing and cold-working experiments. The Cu (111) peak is due to the substrate; it is of no interest and has been truncated.

and temperatures corresponding to this degree of transformation are:

Time, min ± 20%	Temp., °C ± 10° C
5	350
40	300
200	250

Other, rather cursory diffractometer work indicates that, initially, the nucleation and growth of the equilibrium phases proceed very rapidly, as a result, presumably, of the abnormal number of lattice defects retained during the quench. Since the quantity and type of defects cannot be controlled (or even estimated) at present, further work on the kinetics has been postponed.

To obtain order-of-magnitude estimates of the effects of cold working, specimens of the alloy were again quenched upon copper strips. Both specimen and strip were then cooled in liquid nitrogen. By means of a small rolling mill, the total thickness was reduced in 10% decrements. Between passes, the specimen and strip were kept at −190° C. Upon examination (at room temperature) in the diffractometer, it was found that decomposition had indeed occurred; a reduction in thickness of ~50% was responsible for roughly the same degree of transformation as shown in Fig. 3.

Discussion

For metals not forming continuous solid solutions, it is predicted[6] that the primary solid solubilities should be increased under non-equilibrium conditions. The question arises: What factors limit the metastable solubility of one component in the other?

The data cogently suggest, in the author's opinion, that the metastable primary solid solubility of germanium in silver is limited by the same factors operative at equilibrium when restrictions due to, say, disparity in the size of the atoms are unimportant. If it can be assumed that the lattice parameter varies linearly with composition through the whole region (and this relation holds empirically for the majority of other, similar alloy systems), the " terminal " composition is found to be 13·0 ± 1·0% germanium (Fig. 1). For alloys of slightly greater germanium content, the lattice parameter of the f.c.c. structure is, within experimental error, the same −4·0910 ± 4 Å—as that of the " terminal " alloy. Assigning the conventional valences, this limiting composition would correspond to an $e/a = 1{\cdot}39 \pm 3$, a value which has been given considerable theoretical foundation.[4]

The inability, in general, to obtain specimens containing only a single structure (Table I) is to be emphasized. However, Barrett's work[7] on stacking faults may be of pertinence here. He argues that the faulting tendency should be high for supersaturated phases in a two-phase (equilibrium) field in which two close-packed structures coexist. The stacking-fault energy of the alloys considered here should be very low, perhaps of the order of 1 erg/cm².[8] Pronounced faulting is thus possible. Barrett further suggests that the plastic deformation accompanying the (solid-state) quenching may initiate the faulting. For alloys quenched from the liquid state, growth " mistakes " during solidification are probably also involved. Experimental verification of the hypothesized faulting could most readily be obtained by transmission electron microscopy.

Attention is directed to the 16·8% germanium alloy; uncombined germanium has been detected in the quenched alloy, as well as a low-angle unidentified line. However, a change in intensities, as noted for alloys containing the h.c.p.′ structure, has not been observed. Possibly, decomposition has proceeded further, at room temperature, in this alloy than in the adjoining alloys. If so, this might suggest that the unidentified lines are associated with the decomposition.

As mentioned above, the h.c.p.′ structure appears to coexist with germanium throughout the region ca. 20 — 100% germanium. The exact nature of this structure, taking into account the change in intensities and extra diffraction lines, has yet to be determined. The situation is further complicated by the lack of knowledge concerning stacking faults, vacant lattice sites, and possible intermediate decomposition products.

Acknowledgements

Professor Pol Duwez contributed some useful suggestions, as did R. H. Willens. Support was jointly provided by the U.S. Office of Naval Research and the U.S. Atomic Energy Commission.

References

1. Pol Duwez, R. H. Willens, and W. Klement, Jr., *J. Appl. Physics*, 1960, **31**, 1137.
2. M. Hansen and K. Anderko, " Constitution of Binary Alloys ". **1958**: New York and London (McGraw-Hill).
3. E. A. Owen and V. W. Rowlands, *J. Inst. Metals.*, 1940, **66**, 361.
4. W. Hume-Rothery and G. V. Raynor, " The Structure of Metals and Alloys ". **1956**: London (Inst. Metals).
5. Pol Duwez, R. H. Willens, and W. Klement, Jr., *J. Appl. Physics*, 1960, **31**, 1136.
6. See, e.g. L. S. Darken and R. W. Gurry, " Physical Chemistry of Metals ". **1953**: New York and London (McGraw-Hill).
7. C. S. Barrett, " Imperfections in Nearly Perfect Crystals ", p. 97. **1952**: New York and London (John Wiley).
8. P. R. Swann, private communication.

The statements made therein remain yet valid. In addition, low angle hcp′ diffraction lines were detected with the germanium-rich phase in alloys containing as little as 5 at.% Ag. As reported in the preliminary communication[35], the solid solubility of silver in germanium appears to be very small.

Proceeding from the results obtained in the Ag-Ge system, the homologous[17] alloy systems Ag-Si, Au-Ge and Au-Si were investigated. For Ag-Si, it could not be established whether the primary solid solubility could be extended and there was some indication of a metastable hcp phase (cf. III.C.b.). For Au-Ge, lattice spacing measurements did not seem to indicate any appreciable extension of primary solid solubility; however, very complex nonequilibrium structures, as yet unravelled, were found in quenched alloys. For Au-Si, equally complex nonequilibrium structures were found in many alloys but, more importantly, noncrystalline structures were occasionally obtained[36]. This seemed to have been the first time that noncrystalline structures were obtained in metallic alloys by cooling from the melt and the results have already been used by Cohen and Turnbull [37] [38] in their theory of glass formation.

d. Various data for Ag-Cu, Cd-Zn alloy systems

In order to attain any semblance of understanding of the solidification process, the properties of both the liquid and

solid state must be considered, especially in the vicinity of the melting points. Much of the available data of pertinence is here assembled; where experimental results are lacking, estimates of the quantities of interest are made. Some data for the component elements in the Ag-Cu, Cd-Zn alloy systems are given in the following table[39][40][7].

	Ag	Cu	Cd	Zn
At melting point: T(^{o}K)	1234	1356	594	693
ΔH_f heat of fusion (kcal/mole)	2.69	2.84	1.50	1.74
ΔS_f entropy of fusion (cal/mole^{o}K)	2.18	2.09	2.53	2.51
ΔV change (%) in volume	3.8	4.15	4.7	4.2
Coordination number at distance in Å liquid	8-11		8 at 3.06 4 at 4.0	11 at 2.94
solid	12 at 2.89	12 at 2.55	6 at 2.97 6 at 3.29	6 at 2.66 6 at 2.90
Self-diffusion (solid)				
D_o (cm^2/sec)	0.40	0.20	0.10(⊥) 0.05(∥)	0.58(⊥) 0.13(∥)
Q (kcal/mole)	44.1	47.1	18.2(∥) 19.7(⊥)	21.8(∥) 24.3(⊥)

Lumsden[41] has given a thorough discussion of the rather high quality thermodynamic data available for the Cd-Zn system. Since it is of interest to attempt an estimate of the miscibility gaps in the undercooled liquid alloys, the pertinent information for Cd-Zn is that the excess heats of solution are:

$$\bar{H}_{Zn} = 2000\ N^2_{Cd}; \qquad \bar{H}_{Cd} = 2000\ N^2_{Zn}$$

in cal/mole, with N_i the atomic fraction of i; there does not seem to be any excess entropy.

For Ag-Cu, Edwards and Downing[42] have published some data which apparently differ considerably from that in a preliminary report; the latter was used by Kubaschewski and Catterall[43], who arrived at somewhat different estimates for the various quantities. According to the later results[42], both positive excess heats of solution and excess entropies exist but diminish with decreasing temperature. Despite considerable scatter in the data, the excess heats of solution at 1428°K are crudely estimated by the present investigator as:

$$\bar{H}_{Cu} \approx 3400\ N^2Ag, \text{ and from the Gibbs-Duhem equation,}$$
$$\bar{H}_{Ag} \approx 3400\ N^2Cu$$

An overestimate of the temperature of unmixing results if the temperature variation and excess entropy are neglected

but this is done. According to the model employed by Nakagawa[44], the temperature at the boundary for composition N is:

$$T = \frac{W}{R} \left\{ \frac{1-2N}{\log \frac{1-N}{N}} \right\}$$

with $\frac{W}{R} \approx 1000$ for Cd-Zn and 1700 for Ag-Cu. The (symmetric) values obtained are:

Cd-Zn

N	T(°K)	T(°C)
0.5	500	277
0.4	494	221
0.3	470	197
0.2	431	158
0.1	364	91
0.05	305	32

Ag-Cu

0.5	850	577
0.4	840	567
0.3	799	526
0.2	733	460
0.1	619	346
0.05	519	246

Temperature dependencies of the viscosities of liquid metals have been shown to be described quite well by expressions of the form

$$\eta = A \exp \left(\frac{Q}{RT} \right)$$

Gebhardt and coworkers[45] have measured the viscosities at different temperatures for a number of elements and some alloys. To estimate D, the Stokes-Einstein relation may be a fair approximation[46], viz.

$$D = \frac{kT}{6\pi\eta r}$$

where r is taken to be the ionic radius[47] and linearly interpolated values are used for the alloys. The measured and estimated quantities are collected in the following table:

		η (centipoises)		r(Å)	D(cm^2/sec)	
	Q(kcal/mole)	at 1052°K	at 841°K		at 1052°K	at 941°K
Cu	8.6	.36	.55	0.96	2.22×10^{-4}	1.16×10^{-4}
23 at.%Ag;Cu	5.5	.31	.43	1.03	2.40	1.39
35 at.%Ag;Cu	5.4	.29	.40	1.06	2.50	1.45
63 at.%Ag;Cu	4.9	.28	.37	1.14	2.41	1.46
84 at.%Ag;Cu	4.9	.27	.36	1.21	2.36	1.41
Ag	4.9	.26	.36	1.26	2.34	1.35
		at 539°K	at 431°K		at 539°K	at 431°K
Cd[48]		.29	.43	0.97	1.40×10^{-4}	0.76×10^{-4}
Zn		.27	.37	0.74	1.96	1.15

There have been no systematic studies of the undercooling possible in these alloy systems with, say, the standard

small droplet technique. Turnbull[22] has obtained undercoolings of 227°C for Ag and 236°C for Cu. Sundquist[23] found undercoolings to 726°C and 750°C for 36 at.%Cu;Ag and 43 at.%Cu;Ag alloys, respectively. Undercoolings for Cd-Zn alloys on both sides of the eutectic seemed to be small[49].

Turnbull[22] estimated the liquid-solid interfacial energy, σ_{LS}, as 128 ergs/cm^2 for Ag and 189 ergs/cm^2 for Cu; similarly, the present investigator obtained 60 ergs/cm^2 for Cd and 91 ergs/cm^2 for Zn.

Estimates of the free energy vs composition curves for the solid alloys are made at the eutectic and 0.8 eutectic temperatures with Hardy's "subregular" model[50]. Using experimentally determined phase boundaries and assuming no entropies other than those of mixing, the model employs equations of the form:

$$\Delta F = A_1 x^2(1-x) + A_2 x(1-x)^2 + RT\{x\log x + (1-x)\log(1-x)\}$$

where x is at.% solute and $A_1 = 6620, A_2 = 4640$ cal/mole for Ag-Cu and $A_1 = 3800$, $A_2 = 4540$ cal/mole for Cd-Zn. The differences in free energy between solid solutions and stable two-phase alloys at the eutectic and 0.8 eutectic temperatures are plotted vs composition in Fig. 14. These estimates may be within 20% since the "subregular" model allows only for asymmetric solid solubilities but not for

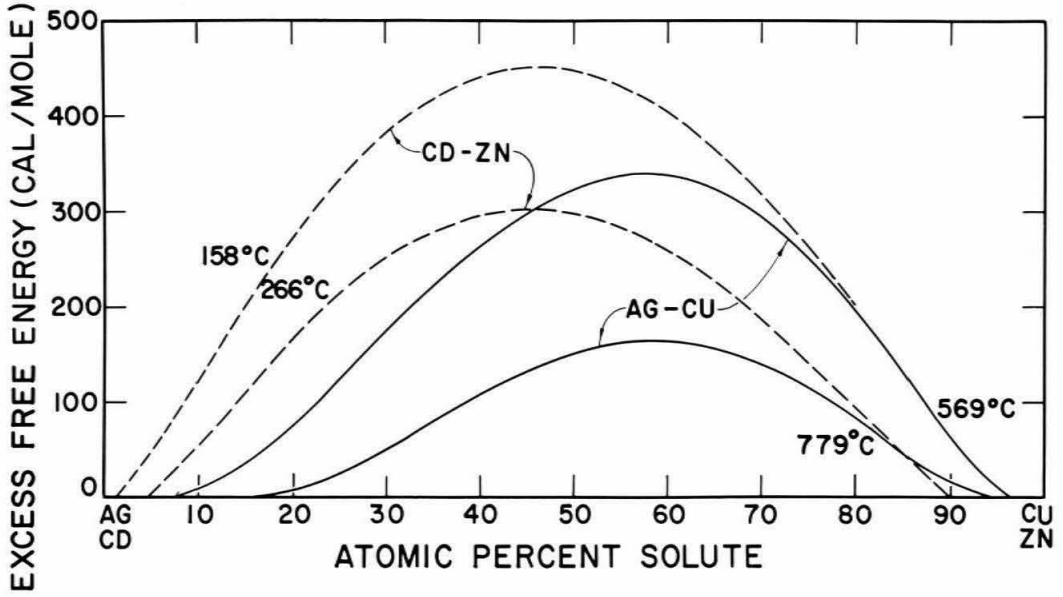

Figure 14. Difference in free energies between metastable solid solutions and equilibrium phases for Ag-Cu and Cd-Zn alloys at eutectic and 0.8 eutectic temperatures as function of composition according to the model of Hardy.

excess entropies, which may be present. Gross errors are to be expected from this model at temperatures far removed from the eutectic.

Neglecting excess entropies, temperature dependencies of entropies of fusion, excess enthalpies, and specific heats as well as the limited solid solubilities, the driving free energies for solidification for equiatomic Cd;Zn and Ag;Cu melts are obtained at the eutectic and 0.8 eutectic temperatures from the above data. For the Cd-Zn alloy, the negative free energy for solidification into the equilibrium two-phase configuration is approximately twice that for the metastable solid solution; for the Ag-Cu alloy, the relative differences are $\sim$10% and $\sim$20% at the eutectic and 0.8 eutectic temperatures, respectively.

There exist no reasonable approximations for the various diffusion-related phenomena in non-dilute solid solutions[40]. However, diffusion coefficients may be within a few orders of magnitude of the self-diffusion coefficients (bulk) computed at the various temperatures of interest, viz.:

$D(cm^2/sec)$

	melting point	eutectic	0.8 eutectic	room	liquid nitrogen
Ag	6×10^{-8}	3×10^{-10}	10^{-13}	10^{-32}	---
Cu	5×10^{-8}	4×10^{-10}	10^{-14}	10^{-34}	---
Cd	10^{-9}	2×10^{-10}	3×10^{-12}	3×10^{-16}	10^{-53}
Zn	2×10^{-9}	2×10^{-11}	10^{-12}	10^{-17}	10^{-63}

D. DISCUSSION

Ideas in the following areas are reviewed with respect to their possible pertinence and validity in the present work -- liquid alloys, especially undercooled liquids; homogeneous and heterogeneous nucleation of solid phases from the melt; growth of the nucleated phases; solid state reactions, especially precipitation. The speculations and ideas of previous workers in the present area of rapid solidification, as presented in III.A., are dealt with. Interspersed throughout are other results from the present experiments; conclusions are tentative and designed to encourage further experiments, as is appropriate for a frankly exploratory investigation.

From the few measurements[51] that have been made, many properties of undercooled liquid alloys seem to be smooth extrapolations of those properties in the equilibrium region. Assuming no appreciable excess entropies, the multicomponent

liquids tend to unmix or order according to whether the enthalpy of mixing is positive or negative, respectively. Unmixing of undercooled liquid alloys has been observed by Nakagawa[44] (Cu-Co and Cu-Fe alloys) under nearly static conditions. Whether unmixing or the tendency thereto, i.e., clustering of like atoms into small groups, can occur under more dynamic conditions -- such as in the present experiments -- has not been directly determined.

Critical in this matter are the diffusion rates in the liquid alloy. According to Nachtrieb[46], the simple picture of atoms jumping from place to place, which suffices to describe diffusion in the crystalline solid, is not valid for the liquid state in which a rapid, collective shifting of groups of atoms is a preferable idealization. Such a model has not proved particularly amenable to calculation; measurements suggest[46], however, that the Einstein-Stokes relation provides a fairly good connection between D and the readily measured η . As estimated for the Ag-Cu and Cd-Zn alloys (III.C.d.), D varies between 1 and 2 x 10^{-4} cm^2/sec over the temperature range of interest. Thus the mean diffusion length $\langle l \rangle \approx \sqrt{4Dt}$ is, for times of order 10^{-4} sec, $\sim 10^{-4}$ cm or 10^4 Å. Thus it seems that the microscopic diffusion processes in the liquid are not sensibly affected by the present rates of cooling. Therefore, inside or near a solubility gap in the undercooled liquid, it is difficult to see how clustering on at least a microscopic

scale can be prevented. It has not been possible to obtain extensive metastable solid solutions in those systems in which a region of liquid immiscibility occurs at equilibrium, e.g., Al-In, Cu-Pb, and also those systems in which unmixing of the slightly undercooled liquid is expected, e.g., Cu-Bi, Ag-Bi, Ag-Pb and Cd-Zn. It is, therefore, suggested that a necessary but not sufficient condition for the extension of solid solubility by rapid solidification (and concomitant undercooling) be that the liquid is not cooled or undercooled into an equilibrium or metastable solubility gap.

Because direct measurements are lacking and perhaps impossible, it is necessary to estimate the magnitudes of the undercoolings sensibly possible in given alloy systems. The slowest step in crystallization from the metallic melt is the nucleation of the solid phase(s) and not the subsequent growth from the liquid. As the process of nucleating a homogeneous solid phase is usually visualized[21][22], the bulk free energy driving force for crystallization below the melting point is opposed by the work necessary to create the surface between the solid and the liquid. At large undercooling, the rate of creation of nuclei of critical radii is very great. Experimentally it has been shown[22], under nearly static conditions, that $\backsim$ 20% undercoolings were the approximate limits for metallic elements. For aluminum solidified under dynamic conditions, Falkenhagen and

Hofmann[2] found similar limits, and likewise for the Cu-Ni[22] alloys which exhibit continuous equilibrium solid solubility.

Except under very refined static conditions, e.g., the small droplet technique[22], homogeneous nucleation is rarely observed. Usually nucleation takes place on an impurity and it has been stated[22] that as little as 1 part in 10^{16} of impurity can cause perceptible heterogeneous nucleation under the typical static conditions. The formal theory of heterogeneous nucleation[21][22] assumes the formation of one type of nuclei and then presumes to delineate the conditions for the nucleation of the other phase(s) upon the initially formed solid. Sundquist[23], studying heterogeneous nucleation in binary alloys with the small droplet technique, has recently shown many of the assumptions of the theory to be inadequate. Retaining the original assumption of the initial formation of one class of nuclei, he proposed a "nucleation series" to rationalize his observations. Elements high in the series (see below) are readily nucleated by those elements lower in the series and pronounced undercoolings are not possible. The elements high in the series (low entropy of fusion) are poor nuclei for those below. Some ambiguities were noted, though, and the generality of the conclusions is uncertain.

	Element	Entropy of fusion (cal/mole°K)
	Tl	1.78
	Pb	1.81
not necessarily in this order	Ag	2.18
	Au	2.28
	Cu	2.09
	Ni	2.44
	Co	2.12
	Fe	2.01
	Ge	5.93
	Sn	3.32
	Zn	2.51
	Bi	4.83
	Sb	5.25

Other experiments[52], under nearly static conditions, suggested that the initially formed nuclei may reproduce themselves rather than be solely occupied with nucleating the other phase(s). Thus, the formal theory of heterogeneous nucleation, which is rather successful in describing aspects of other transformations, is not adequate in the case of the liquid-solid transformation. The present results, e.g., Ag-Cu and GaSb-Ge, suggest, further, that the assumption of one class of nuclei forming originally may also be questionable, at least in the limit of very high cooling rates.

The nucleation phenomena in the present work are poorly understood but, nevertheless, some essentially qualitative ideas are advanced. Fundamental to the development is the previous conclusion that, despite the rapid rate of cooling, the diffusion processes are much faster in the liquids and equilibrium is more nearly approached at all temperatures.

It is assumed that the situation in the undercooled liquid is describable by the classical theory of homogeneous nucleation[22], viz., a sharp interface exists between the liquid and solid nucleus, which are taken as uniform in composition; recent suggestions[53][54] of nuclei with diffuse interfaces and compositional gradients are presently being subjected to experimental examination[55] and do not now seem to be preferable to the classical theory. For nuclei of critical radii $\underline{r}^*$,

$$r^* = \frac{-2\sigma_{LS}}{\Delta G_v}$$

where σ_{LS} is the liquid-solid interfacial energy and ΔG_v is the bulk free energy driving force for solidification. Few measurements exist for σ_{LS}. Another important quantity is ΔG^*, the free energy barrier for a nucleus of critical radius, which is

$$G^* = \frac{K \sigma_{LS}^3}{(\Delta G_v)^2}$$

where K is a geometrical factor. Furthermore, a free energy of activation, ΔG_A, is postulated, which determines the rate

of movement of atoms across the interface through the usual expression from absolute rate theory. The rate of formation of nuclei, I, is then

$$\log I = \log K_v - \frac{(\Delta G^* + \Delta G_A)}{kT}$$

where K_v is an almost temperature-independent factor involving, among other quantities, the size of the nuclei. Unknown here is ΔG_A which is, however, usually taken as $\sim kT$. Unfortunately, the frequency of movement of atoms across the interface and consequently the transient rates of nucleation are exponentially sensitive to ΔG_A. Usually, it is assumed that $\Delta G^* >> \Delta G_A$. Transients[22] are probably not of importance since nuclei of $\sim 10^7$ atoms are required at the $\Delta G_A \sim kT$ and it does not seem likely that such large nuclei are involved.

Jackson and Chalmers[20] have developed an alternative model of the solidification (and nucleation) processes in which the net rate of the process is obtained from the difference in the rates of freezing and melting, as considered independently. For undercoolings of $\sim$ 20%, it was estimated that critical nuclei contained only $\sim 10^3$ atoms. Jackson[19], in a further elaboration of this approach, specifically sought to treat the Ag-Cu system. Although the applicability seemed somewhat forced, it was suggested that

the equilibrium configuration was a good approximation up to growth rates of 100 cm/sec. This does not seem to be so (as discussed below).

Considering the Ag-Cu results first, it is not clear where in the nucleation process outlined above the metastable solid solutions gain a clear-cut advantage over the equilibrium phases as a result of the present large cooling rates. It is expected that σ_{LS} is less for an equilibrium phase and, of course, $|\Delta G_v|$ is greater for the equilibrium configuration. From the previous estimates of ΔG_v for equiatomic Ag-Cu alloys, it is suggested that perhaps

r^* (metastable solid solution) $\gtrsim 1.15\ r^*$ (equilibrium) for Ag-Cu. It thus appears inescapable that many nuclei of the copper- and silver-rich phases are formed together with the nuclei of the metastable solid solutions. For Cd-Zn, the difference in free energies may be so great that only a negligible number of metastable solid solution nuclei are formed.

For the Ag-Ge alloys, it is tempting to suggest that there is some tendency for short range order in the undercooled liquid, resulting in a σ_{LS} sufficiently lower than that of the equilibrium phases to compensate for the difference in ΔG_v and thus in a reasonable nucleation probability for the metastable hcp phases.

Also demanding attention here are the coexisting fcc and hcp phases in Ag-Ge, Ag-Sn and Ag-Sb alloys. It has been

suggested[56] that the free energy differences between fcc structures and hcp structures of similar dimensions and nearly ideal axial ratio must be small in the (equilibrium) two-phase region. Accordingly, faulting requires energies of only a few ergs/cm^2. Although there seems to be a compositional limitation to the primary solid solution, the close packed structures are much alike in other ways, perhaps with nearly the same σ_{LS}. On this basis, nucleation of the two phases (with usually the same composition) in proportions as detected is a real possibility.

Tacitly ignored thus far are the effects of the impurities inevitably present. In contrast to the static undercooling techniques, dynamic experiments such as the present work and that of Falkenhagen and Hofmann -- seem to be little affected by extraneous matter. For a reasonably dilute amount of impurities of perhaps low nucleating power (a' la Sundquist), it is improbable that enough nuclei could be produced to materially affect the situation before the temperature had decreased sufficiently so that an avalanche of nuclei was brought about.

It is necessary to consider the disposition and effects of the release of the heat of fusion. In the static experiments[22] it has been found that the small droplets were heated up to the solidus temperature during this period of recalesence in the initial stages of solidification; Falkenhagen and Hofmann found similar behavior. It is not

clear how much the undercooling persists as solidification proceeds. The rough estimate (App. II) suggests $10^{-6.5\pm0.5}$ sec for the release of heat and solidification; a more realistic number is perhaps 10^{-5} sec. As estimated from the equilibrium bulk diffusion data, $\langle 1 \rangle$, at the Ag - Cu eutectic temperature, is then only $\sim 10\text{Å}$ for the latter time interval, although, in reality, it must be somewhat larger due to the excess vacancies, etc. Movements of similar magnitude may be expected in the solid as it cools on the substrate. However, these matters are inextricably bound up with the processes of growth of the solid phase(s) from the melt.

To make connections between the present work and the body of experience[57][58] amassed for growth under more leisurely and controllable conditions, it seems to be necessary to understand the morphologies of the solidified materials. The grain sizes are, however, usually too small to allow optical examination and electron microscopy is clearly required.

It has been long realized that the growth rates of solid nuclei in undercooled liquid metals are very high and, indeed, may vary as the square of the undercooling[59]. Difficulties in measurement have prevented the establishment of any sensible upper limit, save that implied by the need for a supply of atoms by diffusion in the liquid. The model

of Jackson and Chalmers[20] suggests $\sim$ 200 cm/sec as an upper limit for the present temperature range. Macroscopically it is expected that the growth rates in the present experiments are $\sim 10^2$ cm/sec. Grain sizes are relatively small because of the abundance of nuclei produced homogeneously in the undercooled liquid adjoining the substrate or produced heterogeneously (but not epitaxially) by the substrate. Gellar and Garbeck[60] have undercooled liquid metallic alloys encapsulated in slags and found that fine grain sizes were associated with pronounced undercoolings; this was also apparent from the microstructures presented by Sundquist in his thesis[23].

Despite the quantitative deficiencies in the understanding of the growth processes, some qualitative arguments are possible. For the Ag-Cu alloys, it seems inescapable that a good many nuclei of the equilibrium phase(s) are created along with those of a composition approximately that of the liquid. However, it is plausible that the growth rates of the metastable nuclei are much greater than those of the nuclei of nearly equilibrium composition since the latter are selective in the choice of atoms supplied by the liquid while the former accept atoms indiscriminately. The process is thus visualized as a competition between the various species. For the Ag-Ge, Ag-Sn and Ag-Sb alloys, it seems likely that the growth rates of the fcc and hcp phases are

about the same. Because of the low faulting energies expected, it is not improbable that "mistakes" during growth are also involved. Thus different, but similar structures of the same composition can be rationalized in this way, with implications perhaps of applicability to other pairs of closely related structures. For the structures in Ag-Ge alloys, it is likewise reasonable that the growth rates of the metastable hcp phase are much greater than those of the equilibrium phases.

Upon further cooling of the solidified alloy and its subsequent examination and maintenance at room (or liquid nitrogen) temperature, there is the possibility that the metastable structures thus far retained might anneal out and decompose to some transition structure or to the equilibrium structures. With the present technique, it is reasonably expected that many lattice defects, such as vacancies and perhaps interstitials, have been retained in the quench. Thus diffusion rates are enhanced[61]; also the relatively large proportion of grain boundaries and the possibility of mechanical deformation during the quench would tend to promote diffusion over and above that expected from the equilibrium bulk parameters. Because of the uncertainties in these quantities due to the inability to sufficiently control the quenching technique, it is difficult to assess their participation in the solid state reactions. An attempt to study the kinetics of decomposition of quenched 60 at.%Ag;Cu

alloys was unsuccessful because of the inability to obtain reproducible results due to the variable initial conditions. The initial stages of the decomposition were more rapid because of the hypothesized abundance of lattice defects. It was expected that precipitation would occur more readily at the grain boundaries although nuclei of the equilibrium phases, retained in the quench, would have been fairly potent in the transformation. Until the conditions of the quench can be controlled, kinetics work will remain qualitative.

The results obtained for the Ag-Cu alloys (III.C.a.) apparently require interpretation both in terms of the competition in nucleation and growth and in terms of precipitation.

With the bulk of the present experience and ideas now set forth, it is appropriate to attempt to make the connections between it and the previous work referred to in III.A. Cech's results, which could not be obtained with the present technique, are indeed striking but do not seem to be compatible with the present experience. In no case of structures of high symmetry has it been possible to obtain a given (adjacent) phase by quenching into the equilibrium single-phase field of another phase. As outlined above, the thermodynamic disadvantages in nucleation must be overcome by a significant disparity in growth rates in order to obtain an appreciable amount of the metastable phase. In general, one has to quench into (equilibrium) multi-phase regions to

accomplish this.

Pawlek's success in suppressing complex, peritectic phases opens readily two avenues of investigation; although peritectic structures are unambiguously defined, notions of complexity are less restricted. The peritectic compound Au_2Bi was almost completely suppressed in one rapid quenching experiment and there is promise that many peritectic phases can be prevented in this way. With respect to complex structures, it did not seem that the ϵ-phase in Cu-Si alloys (76 atoms/unit cell) was completely suppressed by rapid quenching; on the other hand, the congruently melting $AuTe_2$ compound did not form upon rapid solidification[62]. No clear cut criteria have emerged thus far.

The use of metastable phase diagrams is perhaps justified in terms of convenience in the approximate representation of nonequilibrium situations under clearly understood conditions. There is no firm physical basis for such representations and indiscriminate use can (and has[18]) lead to absurd interpretations of data. Nothing in the course of the present work seems to have indicated or justified representation by means of a metastable phase diagram.

Three interesting suggestions have come from Falkenhagen and Hofmann[2]. First is the observation that solid solubilities were extended most appreciably in those alloys in which extensive undercooling was noted. This theme is amply

exploited in the interpretation of the present results. However, the paucity of data for liquid alloys and the ignorance concerning nucleation processes do not allow definite predictions of undercoolings in given systems. Another useful correlation is that of the high "ablösearbeit" in Al-Mn alloys and the extension in solid solution therein obtained. It seems that this is related to the persistence of the metastable phase after nucleation and especially during recalescence. That is, if the diffusion rates in the solid are low, there is less likelihood of the metastable structures annealing out in the critical, high temperature interval after nucleation. Since measurements and/or estimates of diffusion rates in solid alloys are generally unavailable, it is doubtful whether this criterion is of practical applicability in the search for metastable structures. Also mentioned was the tendency for extensions in solid solubility to be associated with the presence of intermetallic phases of high melting points. Few systems of this sort were encountered in the present work; also to be realized is that the slight increases in solid solubility, such as formed the bulk of the F-H results (III.A.), were not bothered with here.

Salli and Miroshnichenko[18] carried some of the German ideas somewhat further -- and perhaps too far. The low diffusion rates inferred from the high "ablösearbeit"

results in "crystallization without diffusion," according to the Russians. Also deserving of incredulity are their statements that the undercoolings in several simple eutectic systems were reflected by the less-than-maximum solid solubilities of the resultant phases. In agreement with the present conclusions are the ideas that nuclei of both the stable and metastable phases exist and that the observed structures were a consequence of the competition in growth of the various nuclei. Sufficient evidence is at hand from the Ag-Cu alloys studied to refute the contention[3] that slightly supersaturated solid solutions decompose more rapidly than more strongly supersaturated ones. This contention, however, may be valid for some particular systems though, since fundamental criteria are absent. Of considerable interest in the Russian work was the observation that a spectrum of structures -- from metastable solid solution to equilibrium phases -- was revealed by examination of successive layers of the quenched materials. This is hard to believe since growth once initiated, presumably near the substrate, should be sufficiently rapid to overwhelm the other, different nucleation processes occurring in the interior of the sample. One wonders if the decomposition products noted were not a product of the etching and polishing prerequisite to the metallographic examination. This point, as well as the several others cited above, is deserving of further experimental investigation.

REFERENCES

1. A.U. Seyboldt and J.E. Burke, Procedures in Experimental Metallurgy, (1953).

2. G. Falkenhagen and W. Hofmann, Z. Metallkunde, (1952), 43, 69-81.

3. I.V. Salli, Zhur. Neorg. Khim., (1958), 3, 142-159.

4. R.B. Pond, U.S. Patent 2,825,108.

5. L. Brewer, UCRL 653; as quoted in reference 1.

6. J.W. Taylor, Progress in Nuclear Energy, (1959), V2, 398-416.

7. A. Bondi, Chem. Rev., (1953), 52, 417-458.

8. G.L.J. Bailey and H.C. Watkins, J. Inst. Metals, (1951-2), 80, 57-76.

9. E.R. Parker and R. Smoluchowski, Trans. ASM, (1945), 35, 362-373.

10. H.-L. Luo, private communication.

11. L. Marton, Methods of Experimental Physics - Solid State Physics, (1959), 6B, 61.

12. S. Sekito, Z. Krist., (1930), A74, 189-201.

13. R.E. Cech, Trans. AIME, (1956), 206, 585-589.

14. A.K. Covington, K. Groenwolt and B.W. Howlett, J. Inst. Metals, (1960-1), 89, 291-2.

15. F. Pawlek, Z. Metallkunde, (1944), 36, 105-111.

16. J. Schramm, Ibid., 111-112.

17. M. Hansen and K. Anderko, Constitution of Binary Alloys, (1958).

18. I.V. Salli and I.S. Miroshnichenko, Doklady Akad. Nauk SSSR, (1960), 132, 1364-1367.

19. K.A. Jackson, Can. J. Phys., (1958), 36, 683-691.

20. K.A. Jackson and B. Chalmers, Can. J. Phys., (1956), 34, 473-490.

21. D. Turnbull, Thermodynamics in Physical Metallurgy (ASM), (1949), 282-306.

22. J.H. Holloman and D. Turnbull, Progress in Metal Physics, (1953), 4, 333-388.

23. B.E. Sundquist, Thesis - Illinois Inst. of Tech., (1960).

24. W.B. Pearson, Handbook of Lattice Spacings and Structures of Metals and Alloys, (1958).

25. G.A. Busch and R. Kern, Solid State Phys., (1960), 11, 1-40.

26. H. Lipson and A.R. Stokes, Nature, (1941), 148, 437.

27. A. Schneider and G. Heymer, Z. anorg, Chem., (1956), 286, 118-135.

28. W. Hume-Rothery and G.V. Raynor, The Structure of Metals and Alloys, (1956).

29. E. Raub and M. Engel, Z. Elektrochem., (1943), 49, 89-97.

30. H.H. Chiswik and R. Hultgren, Trans. AIME, (1940), 137, 442-446.

31. E. Raub and A. Engel, Z. Metallkunde, (1946), 37, 76-81.

32. E. Raub and A.V. Polaczek-Wittek, Z. Metallkunde, (1942), 34, 93-96.

33. R.D. Heidenreich, Acta Met., (1955), 3, 79-86.

34. E.A. Owen and E.W. Roberts, Phil. Mag., (1939), 27, 294-327.

35. P. Duwez, R.H. Willens and W. Klement, J. Appl. Phys., (1960), 31, 1137.

36. W. Klement, R.H. Willens and P. Duwez, Nature, 187, (1960), 869-870.

37. M.H. Cohen and D. Turnbull, Nature, (1961), 189, 131-132.

38. D. Turnbull, Trans. AIME, (1961), 221, 422-439.

39. B.R.T. Frost, Progress in Metal Physics, (1954), 5, 96-142.

40. D. Lazarus, Solid State Phys., (1960), 10, 71-127.

41. J. Lumsden, Thermodynamics of Alloys, (1952).

42. R.K. Edwards and J.H. Downing, J. Phys.-Chem., (1956), 60, 107-111.

43. O. Kubaschewski and J.A. Catterall, Thermochemical Data of Alloys, (1956).

44. Y. Nakagawa, Acta Met., (1958), 6, 704-711.

45. E. Gebhardt and K. Kostlin, Z. Metallkunde, (1958), 49, 605-613.

46. N.H. Nachtrieb, Liquid Metals and Solidification (ASM), (1958), 49-86.

47. C. Kittel, Introduction to Solid State Physics, (1953), 40-41.

48. K. Gering and F. Sauerwald, Z. anorg. Chem., (1935), 223, 204-208.

49. B.E. Sundquist, private communication.

50. H. Hardy, Acta Met., (1953), 1, 202-209.

51. G. Urbain; G. Cavalier, The Physical Chemistry of Metallic Solutions and Intermetallic Compounds, Vol. I & II, (1960).

52. L. Benjamin and R.F. Strickland-Constable, Acta Met., (1960), 8, 362-372.

53. J.W. Cahn and J.E. Hilliard, J. Chem. Phys., (1958), 28, 258-267.

54. J.W. Cahn and J.E. Hilliard, J. Chem. Phys., (1959), 31, 688-699.

55. B.E. Sundquist and R.A. Oriani, J. Chem. Phys., (in press).

56. C.S. Barrett, Imperfections in Nearly Perfect Crystals, (1952), 97.

57. K.A. Jackson, Liquid Metals and Solidification (ASM), (1958), 174-186.

58. J.W. Rutter, Ibid., 243-275.

59. G.A. Colligan and B.J. Bayles, Acta Met., (in press).

60. W. Geller and H. Garbeck, Arch. fur Eisenhutt., (1955), 26, 611-621.

61. A. Le Claire, Progress in Metal Physics, (1953), 4, 265-332.

62. H.-L. Luo and W. Klement, J. Chem. Phys., (in press).

63. H.S. Carslaw and J.C. Jaeger, Conduction of Heat in Solids, (1959).

64. L.R. Ingersoll, O.J. Zobel and A.C. Ingersoll, Heat Conduction, (1948), 241-246.

65. N.I. Varich and K.E. Kolesnichenko, Tsvet. Metallurgiya, (1960), 4, 131-137; as quoted in Met. Abstr., (1961), 28, 715.

66. W. Hofmann, Aluminium, (1938), 20, 865-872.

APPENDIX I: Metastable bcc structures in solidified Fe-Ni alloys

One of the more interesting of the nonequilibrium phenomena in the Fe-Ni system[17] is that investigated by Cech[13] who found bcc phases in alloys containing up to 30 wt.% Ni which had been solidified rather slowly as small spherical particles. Alloys were prepared by the reduction of homogenized oxides which were then heated to above the liquidus in hydrogen and dropped through a vertical furnace, thereby solidifying. For the 30 wt.% Ni;Fe alloy, the powder thus produced was found to contain nearly equal amounts of bcc (δ or α) and fcc (γ) particles, the former being smaller and single crystals and the latter polycrystalline. Further work appeared to indicate that the bcc structures formed directly from the melt and not by the martensitic transformation, $\gamma \rightarrow \alpha$. It was then suggested that the droplets had been undercooled sufficiently so that the bcc phase was preferentially nucleated with some particles transforming to fcc before reaching room temperature. This transformation, $\delta \rightarrow \gamma$, should be favored in larger particles and seemed to be borne out by the experiments. Cech extrapolated the δ -liquidus and solidus into the γ-region and claimed that nucleation of δ from the undercooled liquid could occur in the region thus bounded. The cooling rates were calculated to be $\sim 100^{\circ}C$/sec for a 13 μ particle, but only $10^{\circ}C$/sec for a 4μ particle; there is

some evidence that very small particles would tend to transform to γ because of this relatively slow cooling rate. It was calculated that, upon release of the heat of fusion, the 13μ particle would be held 1/20 sec at the temperature of solidification. To compare results obtained from the present technique with the above, alloys were prepared in alumina crucibles from iron of purity $\geq$ 99.9% and nickel of purity $\geq$ 99.95%. The immediate vicinity of the nozzles was doused with argon to heating the alloys to 1500-1550°C and quenching onto copper. The effects of contamination were strikingly in evidence for two quenched specimens of pure iron; for one, shot from an insert doused with argon, only the bcc (α) was detected with a lattice parameter, $a = 2.8685 \pm 20$Å, in agreement with others[24], while, for the other shot from an undoused crucible, a fcc phase was detected with lattice parameters[24] suggestive of considerable nitrogen contamination. For the 20, 30 and 40 at.% Ni;Fe alloys investigated, a bcc phase was detected only in the 20 at.% Ni;Fe alloy and this was probably due to the martensitic transformation. For the other alloys, only γ-phases were found. Cech's results thus cannot be obtained with the present technique; further comments are given in III.D.

APPENDIX II: Cooling and solidification - macroscopic viewpoints

To obtain rough estimates of the times involved in the various stages of the cooling, the process is idealized as follows:

(a) The geometry is taken to be one-dimensional with a slab of the material of interest (denoted m for metal) abutting a slab of the poorly conducting material (denoted i for insulator) which, in turn, abuts the semi-infinite, perfect heat sink (denoted w for wall). Conduction is the only mechanism considered for heat transfer, which is assumed perfect between regions. Contact resistance at the interfaces, finite thermal conductivity of the wall, etc. is allowed for by variation of the parameters of the poorly conducting layer. Typical ranges of values for the pertinent thermal parameters are considered.

(b) The three stages in the process are:

(i) Cooling of the molten layer, initially at the superheat temperature, ϑ_{sph}, to ϑ_s, the solidification temperature.

(ii) Propagation of the solid-liquid interface through layer m, at ϑ_s, with concomitant release of the heat of fusion.

(iii) Cooling of the solid layer from ϑ_s to ϑ_o, the original temperature of the wall.

Stages (i) and (iii) are treated similarly, with the pertinent equations;

$$\frac{\partial \vartheta_r}{\partial \tau} = K_r \frac{\partial^2 \vartheta_r}{\partial x^2} \qquad \text{where } r = \underline{i},\underline{m}$$

$K_r = \frac{k_r}{C_r \rho_r}$ thermal diffusivity

k_r = thermal conductivity

C_r = specific heat

ρ_r = density

and the boundary conditions:

$$\frac{\partial \vartheta_m}{\partial x}(l_m, t) = 0; \quad \vartheta_m(x,0) = \vartheta_{sph} \ (\text{or } \vartheta_s) \quad 0 < x < l_m$$

$$\vartheta_i(-l_i, t) = \vartheta_s (\text{or } \vartheta_o); \quad \vartheta_i(x,0) = \vartheta_s (\text{or } \vartheta_o) \quad -l_i < x < 0$$

$$k_m \frac{\partial \vartheta_m}{\partial x}^{(0,t)} = k_i \frac{\partial \vartheta_i}{\partial x}^{(0,t)}$$

Separating variables,

$$\vartheta_r \sim (\text{space-dependent function}) \exp \left\{ \frac{-K_r \beta_{rn}^2 t}{l_r^2} \right\}$$

with $\beta_{rn} \sim n^2 \pi^2$ $\quad (n = 1,2\ldots \quad)$

An exact solution can only be obtained numerically; however, from an analogous problem[63], $\vartheta_m (l_m, t)$ is sensibly ϑ_s (or ϑ_o) for

$$\frac{K_r t}{l_r^2} \sim 2 - 4$$

Estimates of the times involved in stages (i) and (iii) are gotten with numbers[64] collected below in cgs units and arranged--- high > probable > low.

K_m $\quad 1.5 > 0.8 > 0.05$

l_m $\quad 2\cdot10^{-3} > 10^{-3} > 5\cdot10^{-4}$

t_m $\quad 6\cdot10^{-3} > 5\cdot10^{-6} > 2\cdot10^{-7}$

K_i $\quad 0.2 > 10^{-2} > 2\cdot10^{-3}$

l_i $\quad 5\cdot10^{-6} > 10^{-6} > 10^{-7}$

t_i $\quad 3\cdot10^{-5} > 3\cdot10^{-8} >$ transit time for sound wave

The poorly conducting layer does not affect the time required for cooling to within an order of magnitude. There is little difference between the time required in stages (i) and (iii), which is taken as $10^{-4.5\pm0.5}$ sec.

For stage (ii), the propagation of a solid-liquid interface into a semi-infinite liquid is considered. This, the so-called Neumann problem, has been discussed elsewhere[62][63]. A particular solution is $x = \gamma t^{\frac{1}{2}}$ where x is the distance of the interface from the wall and γ is of order 1-4 for the present situation. The estimates of the times necessary for the interface to traverse the distance l_m are

$$4\cdot10^{-6} > 3\cdot10^{-7} > 10^{-8}$$

or time required $\sim 10^{-6.5\pm0.5}$ sec.

The overall time required for the coolings and solidification are then,

$$t_{overall} \sim 10^{-4 \pm 1} \quad \text{sec}$$

assuming the validity of the physical parameters and models chosen. For the latter, approximations have been selected which should yield overestimates of the several time intervals.

APPENDIX III: Aluminum-base manganese alloys and very high cooling rates

Several workers have studied the metastable solid solubility of manganese in aluminum by rapid quenching from the melt. Falkenhagen and Hofmann[2], with cooling rates to $\sim 29{,}000^{\circ}C/sec.$, claimed to have obtained solid solutions containing ~ 4.7 at.% Mn, although single-phase alloys were gotten only to ~ 3.6 at.%Mn. Varich and Kolesnichenko[65] have claimed the extension of solid solubility to ~ 5.2 at.% Mn, with cooling rates of $\sim 50{,}000^{\circ}C/sec.$, although lattice parameters were not presented.

Alloys were prepared in alumina crucibles from aluminum of purity $> 99.99\%$ and remelted electrolytic manganese of purity $> 99.9\%$. Weight losses were small and the alloy wires were believed homogeneous to ± 0.3 at.%. Alloy charges were heated to $\sim 1300^{\circ}C$ in alumina inserts and quenched onto copper. X-ray work was done in the usual way although, since CuKα radiation was used for the convenience of short exposures, the background was high and the quality of the films below the usual standards.

The results of the present work are given in Figure 16; also plotted there are the data of Hofmann[66], Falkenhagen and Hofmann[2] and Fridlander (as quoted by Pearson[24]). Faint lines, with d $\sim 2.06\text{Å}$, 2.16Å, 3.80Å, were detected in the multiphase (shaded symbols) high-manganese alloys of the present work.

There is disagreement between the present work and that cited above. The reasons are presently unknown and it is unfortunate that Varich and Kolesnichenko[65] did not present their very recent measurements. The present data was fitted nicely with a linear lattice parameter vs composition relation, of slope -0.009_3 Å/at.% Mn. The extent of the metastable solid solubility was 5.1 ± 0.3 at.% Mn. The fcc spacings in the 8.8 at.% Mn;Al alloy suggested a subsidiary metastable solid solubility limit at ~ 4.3 at.% Mn, near the limit of Falkenhagen and Hofmann.

To bring the present results into agreement with the previous work, a loss of aluminum during the quenching is demanded. This could have resulted from reactions within the alumina insert although there is no evidence for this. Other contamination, pickup of carbon, oxygen, etc., may be involved but hardly to the degree necessary for the gross difference in lattice spacings. At the very least, it is suggested that the cooling rates of the present technique are equal to those claimed elsewhere.

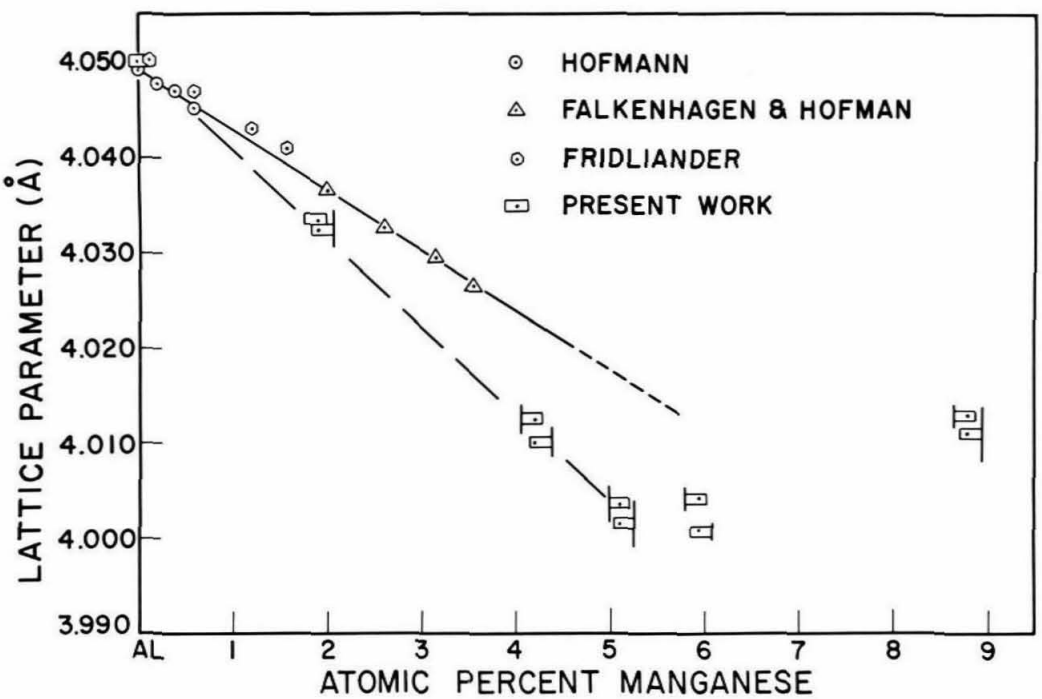

Figure 15. Lattice parameters plotted as function of manganese concentration for face centered cubic structures.